International Journal of Energy Research

INTERNATIONAL JOURNAL OF ENERGY RESEARCH
Int. J. Energy Res. (2016)
Published online in Wiley Online Library (wileyonlinelibrary.com). DOI: 10.1002/er.3598

REVIEW PAPER

Battery state of health estimation: a structured review of models, methods and commercial devices

Lucian Ungurean[1], Gabriel Cârstoiu[1], Mihai V. Micea[1,*,†] and Voicu Groza[2]

[1]Department of Computer and Information Technology, Politehnica University of Timisoara, Romania
[2]School of Electrical Engineering and Computer Science, University of Ottawa, Canada

SUMMARY

Estimating the dynamic status parameters of a battery, such as its state of health (SoH) and remaining useful life (RUL), is still a very difficult and complex task. In this paper we perform a structured review of the most relevant state of the art models, algorithms and commercial devices employed in the estimation of the SoH/RUL battery performance figures, in the context of embedded applications. The models and estimation techniques are thoroughly classified and, for each taxonomy class, a presentation of the working principles is made. A comprehensive set of metrics is then introduced for the evaluation of the SoH/RUL estimation techniques from the perspective of their implementation and operation efficiency in embedded systems. These algorithms are then analyzed and discussed in a comparative manner, with concrete figures and results. The capability and the performance of the different types of off-the-shelf fuel gauges to estimate the battery SoH/RUL parameters are also evaluated in this paper. Copyright © 2016 John Wiley & Sons, Ltd.

KEY WORDS

battery state estimation; state of health; remaining useful life; battery model; embedded application; battery fuel gauge

Correspondence

*Mihai V. Micea, Department of Computer and Information Technology, Politehnica University of Timisoara, Romania.
†E-mail: mihai.micea@cs.upt.ro

Received 28 April 2016; Revised 15 June 2016; Accepted 15 June 2016

1. INTRODUCTION

1.1. Battery monitoring in the context of embedded devices and applications

Efficient gathering, storing and using of electrical energy under severe constraints of volume, weight and cost is a major topic of interest in current science and technology, with direct impact in every field of modern human activity, because of the omnipresence of embedded devices and applications.

Still widely considered as the most feasible solution today, rechargeable batteries are complex electrochemical systems, highly sensitive to internal, external and operating conditions, such as temperature, charging current, discharge profiles and depth of discharge (DoD). Moreover, the battery characteristics and behavior are nonlinear and change significantly over time, because of the 'aging' phenomenon. Therefore, battery management systems (BMSs) are a vital component of modern battery packs, with two major roles [1–3]:

a. to ensure the safe operating area (SOA) of the battery, defined by manufacturing and architecture related specifications, such as the maximum charge and discharge currents, maximum DoD, upper and lower boundaries for the voltage of the individual cells, and
b. to continuously measure battery parameters, to determine or predict its status, health and performance figures—generally referred to as *battery monitoring*.

BMS in general, and battery monitoring in particular, require specialized hardware and software to implement precise measurements of parameters such as voltage, current and temperature, as well as complex data processing and prediction algorithms. Two main categories of status and performance figures of the battery are usually determined by such algorithms: instant status (snapshot) parameters and characteristics related to the dynamic status (history) of the battery.

State of charge (SoC) is a key indication of the instant status of the battery, which estimates the percentage amount of energy it currently stores, relative to the most recent fully charged state. The SoC can provide to the user a rough indication on the time the battery will last until full discharge and, in automotive applications for example, this parameter can be used in a similar way the fuel gauge is in conventional cars. Nevertheless, without information on

Copyright © 2016 John Wiley & Sons, Ltd.

the history of the battery, SoC alone cannot accurately indicate the remaining time until complete discharge. Therefore, the dynamic status figures of the battery are very important in battery monitoring and management systems.

State of health (SoH) is an indication of the dynamic status of a battery, related to the initial condition of the battery. Typically, this initial condition (at the time of manufacture) is considered SoH = 100%. With time and usage of the battery, the SoH will decrease, because of irreversible internal chemical and physical processes generally referred to as battery aging. When the capability of the battery to store and provide energy decreases under a predefined threshold, it is considered depleted (but still further usable) and needs to be replaced. At this point, the SoH is defined as 0%.

Remaining useful life (RUL) is another important parameter, belonging to the same category of dynamic battery status figures. It is directly related to the SoH, as it is generally defined as the number of charge/discharge cycles or the time left until the battery reaches to the SoH = 0%.

Compared to the instant parameter case, estimating the dynamic status parameters of a battery, such as the SoH and RUL, is still a very difficult and complex task. The challenges are further increased by the frequent cases where already used batteries are employed in various applications, such that their previous history is unknown to the battery state and health estimation algorithms. Currently, these techniques still need consistent improvements to meet the efficiency required by most real-life applications, especially in the field of sensors and embedded control.

Aware of the importance and the current problems of this topic, we are investigating and reviewing in this paper the most relevant state of the art models, algorithms and commercial devices employed in the estimation of the SoH/RUL battery parameters and performance figures.

1.2. Related work and motivation of the survey

As an indication of the major interest the embedded, reusable power sources and, in particular, the batteries have gained in late years, stand the impressive number and variety of researches and scientific publications in this area. There are also many surveys which discuss and compare the proposed approaches and results.

An extensive review of the state of the art methods for monitoring and estimating lithium-ion (Li-ion) battery states and parameters is provided in [1]. The approaches from an impressive total of 375 scientific and technical sources are classified into six categories, according to the main battery parameters and performance figures: state of charge, battery capacity, impedance, available power, SoH and RUL. The methods employed within each of these categories are then briefly discussed in a critical manner, with emphasis on their advantages and weaknesses. On the other hand, the techniques under review are very briefly presented or not presented at all. Only the Li-ion batteries (LIBs) are covered regarding battery chemistry. Furthermore, this work takes into consideration only the methods which can be applied to battery electrical vehicles (BEVs) and hybrid electrical vehicles (HEVs). From the same perspective, the authors of [2] review some of the most important advances and challenges regarding BMS for LIBs. A presentation of the SoC, SoH and state of function (SoF) battery state figures is made, along with a discussion of the various techniques proposed in the literature for estimating these parameters. Except for the SoC case, this analysis is relatively short and does not provide concrete results and figures. Similar approaches can also be found in [4–6].

Battery aging process for Li-ion chemistries in automotive application is reviewed in detail in [7] and some techniques for estimating it are then briefly analyzed, mainly from the perspective of their advantages and drawbacks. These methods, which are mainly proposed in the state of the art for the SoH prediction, are roughly classified into five categories: algorithms based on electrochemical and equivalent circuit models, performance-based, analytical methods with empirical fitting and statistical approaches. Other surveys sharing this perspective can be found in the literature, e.g. [8].

With the focus on the same electrical vehicle application area, the authors of [3] review some of the methods for estimating battery SoC and SoH performance figures, as part of the emerging prognostics and health management (PHM) scientific field. Several battery electrical and electrochemical models, such as the Thevenin-based and the runtime-based models, followed by the neural network, support vector machine (SVM), fuzzy logic and Kalman filter data-driven methods, are briefly presented in the context of the SoC and SoH estimation. The corresponding approaches in the literature are discussed in a relatively short and general manner, without performance figures and comparisons. From a similar PHM perspective, the authors of [9] review the various prognostics approaches used in the state of the art to predict the RUL of generic engineered systems, by broadly categorizing them into experience-based, data-driven, physics-based and combined (hybrid) approaches. As a case study, such a hybrid prognostics approach has been applied to estimate the RUL of LIBs, by combining the physics-based standard particle filter state estimation process with two data-driven methods, i.e. the support vector regression (SVR) and a similarity based prediction method.

A survey of the most common physics-based battery modeling techniques is given in [10], for electrical and hybrid vehicle battery chemistries such as the nickel-metal-hydride (NiMH) and Li-ion. The electrical, impedance and electrochemical mathematical models are presented and the related approaches in the literature are briefly discussed.

In [11], Moldovan, Weibelzahl and Hava Muntean focus on the energy-aware mobile learning systems and present, in this context, an overview of three main battery

state and performance parameters, i.e. SoC, SoH and the remaining run time (RRT). Some of the techniques proposed in the field to estimate these parameters are briefly reviewed, especially for the SoC figure. A short presentation of several battery models is also included, based on a classification into five categories: empirical models, electrochemical, electrical-circuit, mathematical and hybrid models.

Motivated by the shortcomings identified in the reviews presented above, the approach proposed in this survey focuses on improving the following aspects which are incompletely treated or even missing from the related papers in the literature:

- An exhaustive classification and presentation of the working principles of the most relevant battery models and SoH/RUL estimation methods currently found in the state of the art
- Introduction of a comprehensive set of metrics, specially selected for the analysis and evaluation of the SoH/RUL estimation techniques from the perspective of their implementation and operation efficiency in embedded systems
- Detailed discussion and evaluation, in a comparative manner, of the battery state and health estimation methods, based on the proposed taxonomy and set of metrics, with concrete figures and results
- An analysis of the current off-the-shelf commercial solutions for the SoH/RUL estimation.

1.3. Synopsis of the paper and intended audience

Using battery models to calculate various parameters and as a base for algorithms which estimate battery health and performance figures is a common approach in the state of the art. In Section 2, we present and discuss the most relevant types of battery models found in the literature. The review is based on a classification of the battery models into four main categories, as shown in Table I.

Battery state and health estimation is a non-trivial task and a large number and variety of methods have been proposed in the literature. A survey of the SoH/RUL estimation methods is made in Section 3, based on a classification of the algorithms employed (see Table II). For each category, we present the underlying theoretical principles, to provide an indication of both the operating foundations of the algorithms, as well as of their required computational complexity. The various methods derived from the basic approach are then discussed, in terms of implementation particularities, accuracy and performance.

Table I. Classification of battery models.

Subsection	Battery models
2.1	Electrical (Randles) models
2.2	Electrochemical models
2.3	Mathematical models
2.4	Lifecycle models

Section 4 contains a structured analysis of all the SoH/RUL estimation methods covered in this survey. We propose a system for the qualitative and quantitative evaluation of these algorithms, composed of six metrics: *battery chemistry*, *computational complexity*, *data processing mode*, *estimation result*, *processing time* and *estimation precision*. The evaluation results are synthetically presented in a head-to-head, detailed comparison table, at the end of this section.

An analysis of the state of the art commercial devices for battery monitoring and state estimation—the battery fuel gauges—is provided in Section 5. A general presentation of the battery fuel gauge is made, followed by a discussion and comparison of such off-the-shelf products, commonly found on the market. The approach is focused on the capability and the performance of the different types of fuel gauges to estimate the battery SoH/RUL figures.

In conclusion, this survey is addressed mainly to scientists and engineers in the field of embedded devices and applications, who are either studying the large variety of recent battery state and health estimation techniques, or searching to select a particular SoH/RUL estimation method for an efficient implementation on embedded targets.

2. BATTERY MODELS

A battery model establishes rules and formulas which can be then used to directly calculate the desired output quantities. It can be also considered as an input on which the SoH and RUL estimation methods are based upon. The process of modeling measured battery parameters in order to obtain estimations of its SoH and RUL has been extensively used in the literature. In this section, we will investigate some of the most relevant battery models in the state of the art.

2.1. Electrical battery models

An electrical battery model can also be referred to as an *equivalent circuit model* (*ECM*), *Randles model* or *Thevenin model*. All ECMs are based on the same structure: an ideal voltage source, a series resistance and one or several resistor-capacitor groups, the groups being connected in series with the resistance.

The ideal voltage source represents the open-circuit voltage of the battery (*OCV*, denoted as U_{OC}) and it is an important input parameter, used in various estimation methods. The series or ohmic resistance (denoted as R_Ω) is the battery internal resistance when applying a constant charge or discharge current. The R_p–C_p pairs, in which the resistance is always connected in parallel with the capacitance, are used for modeling the battery behavior in dynamic operating conditions, e.g. when the current is not constant. They are also used for expressing the battery

Table II. Classification of battery SoH/RUL estimation techniques.

Subsection	SoH/RUL estimation methods
3.1	Coulomb counting
3.2	Open circuit voltage (OCV)
3.3	Electrochemical impedance spectroscopy (EIS)
3.4	Kalman filter based (KF): EKF, DEKF, UKF, SPKF, CDKF
3.5	Support vector machine (SVM)/relevance vector machine (RVM)
3.6	Particle filtering: SIR, RBPF
3.7	Fuzzy logic
3.8	Other methods: least squares, magnetic field, sample entropy, approximation entropy, unobserved model, probability density function (PDF), Gaussian process functional regression, Wiener process, autoregressive model (AR) with particle swarm optimization (PSO), neural network, Bayesian approach

voltage response to a step increase or decrease of the current, as current pulses are used by several parameter estimation methods described in the art. The simple (classic) ECM, which employs a single R–C pair, is presented in [12] (see Figure 1).

In [13] the authors present a solution in which the model parameters are recalculated online at each charge/discharge cycle. Some simplifying assumptions are also made in [12], to aid the calculation of the SoC: R_Ω, R_p and C_p are invariant from 3.0 V to 4.2 V, but they do change with the battery SoH. Another assumption states that the $U_{OC}(SoC)$ is invariant with the temperature and the SoH. The model can be expressed mathematically as:

$$\begin{cases} U = U_{OC}(SoC) + I R_\Omega + U_p \\ I = \dfrac{U_p}{R_p} + C_p \dfrac{dU_p}{dt} \end{cases} . \quad (1)$$

In (1), U_p is the voltage drop across the resistor-capacitor group. This simple ECM is used extensively in the art ([14–16]). An interesting approach to modeling the battery voltage can be found in [17]. Here, an over-simplified Randles model is used, which is comprised of

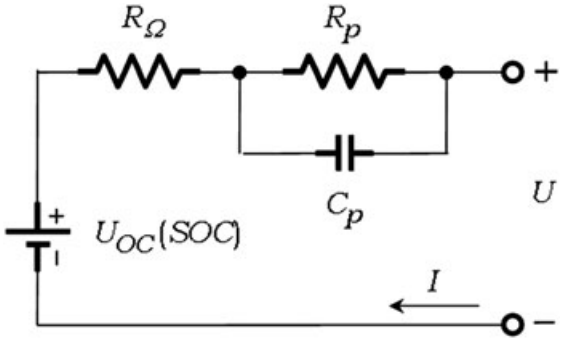

Figure 1. Simple electrical battery model.

only the OCV ideal source and the series ohmic resistance. The authors consider this model to be sufficient for their purposes, because it offers a balance between accuracy and simplicity, and the estimation of the SoC is carried out by using an unscented Kalman filtering approach.

A more complex ECM, which uses two R–C pairs, is described in [18]. The proposed approach is to use one of the R–C pairs for expressing the battery terminal voltage when charging the battery and the other one for modeling the battery voltage during discharge. A similar model has also been described in [19].

2.2. Electrochemical battery models

As variants of the Randles model, these models try to approximate as accurately as possible the chemical processes which take place inside a battery cell of Li-ion class during the charge, discharge and the relaxation phases. From the chemical point of view, the LIB is comprised of three main components: the negative electrode, the separator and the positive electrode. In this model, the Li ions flow from the negative electrode to the positive electrode during discharge, and vice versa during the charging phase ([20,21]).

Figure 2 shows an electrochemical impedance model based on the single particle approach employed in [20]. The impedance of the battery using this model can be expressed as:

$$Z_{batt} = j\omega L + \frac{Z_{n,SEI}}{S_n} + R_0 + \frac{Z_p}{S_p} \quad (2)$$

where $Z_{n,SEI}$ is the impedance of the anode and the solid–electrolyte interface, Z_p is the cathode impedance and S_n and S_p are the surface areas of the anode and the cathode, respectively.

Another variant of a second-order Randles model is employed in [22] for estimating the capacity fade of LIBs, which is essentially the SoH after accelerated aging, not after the actual usage. Although a relatively complex model is used, the authors find that only three out of the eight parameters of the model can be used for the actual estimation.

The electrochemical model can also be applied to other battery chemistries, such as Lead-Acid [23]. In [24] the authors propose a simplified Randles model which they prove to be sufficient for estimating the SoH, based on only one parameter of the model. A more complicated approach is presented in [25–27], where the ion concentration and chemical reactions are modeled using differential functions.

2.3. Mathematical models

The mathematical models generally use one (electrical) battery parameter for the estimation of the SoH. In [28], SoH estimation is done based on constant current–constant voltage (CC–CV) charge curves and calendar aging analysis. For each charge cycle, in the CV phase, the current can be expressed using:

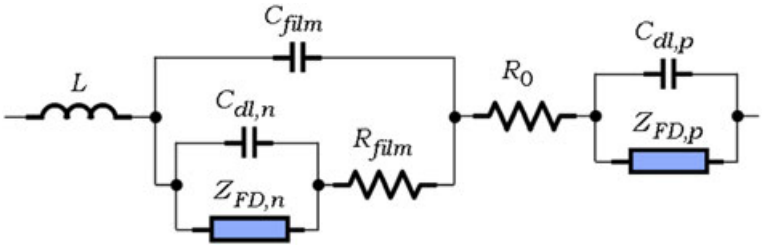

Figure 2. Electrochemical battery model.

$$I(t) = Ae^{-Bt} + C \tag{3}$$

where A, B and C are scalars representing the model parameters. Taking into consideration the dependency of the model parameters on the capacity loss of the battery, (3) can be rewritten as:

$$I(t, C_{loss}) = A(C_{loss})\, e^{-B(C_{loss})\, t} + C(C_{loss}). \tag{4}$$

The authors show there is a linear relationship between the remaining capacity and the value of parameter B: a decrease in battery capacity follows a decrease in the value of parameter B. All the measurements and analysis have been done offline on a significant number of cycles.

In [29] and [30], the OCV mathematical model is employed to determine the SoH based on the incremental capacity analysis (ICA) method. The OCV can be defined as:

$$OCV(z) = K_0 - \frac{K_1}{z} - K_2 z + K_3 \ln(z) + K_4 \ln(1 - z) \tag{5}$$

where $K_{0\text{–}4}$ are the model parameters, and z the normalized SoC. Better estimation results are obtained using a more complex model:

$$OCV(z) = K_0 + K_1 \frac{1}{1 + e^{\alpha_1 (z - \beta_1)}} + K_2 \frac{1}{1 + e^{\alpha_2 (z - \beta_2)}} + K_3 \frac{1}{1 + e^{\alpha_3 (z-1)}} + K_4 \frac{1}{1 + e^{\alpha_4 z}} + K_5 z. \tag{6}$$

The incremental capacity (IC) curves were derived from over 2000 charge/discharge cycles.

In [31], the SoH is predicted from the capacity curves resulted from capacity measurements in each battery cycle. Three prediction models are compared in terms of accuracy: the exponential model (7), the polynomial model (8) and the proposed ensemble model (9):

$$C_{Ak} = C_{Ak1} + C_{Ak2} = \alpha_1 e^{\alpha_2 k} + \alpha_3 e^{\alpha_4 k} \tag{7}$$

$$C_{Bk} = C_{Bk1} + C_{Bk2} = \beta_1 k^2 + \beta_2 k + \beta_3 \tag{8}$$

$$C_{Ck} = \gamma_1 e^{\gamma_2 k} + \gamma_3 k^2 + \gamma_4 \tag{9}$$

where C_{Ak}, C_{Bk} and C_{Ck} are the values of the battery capacity, k represents the discharge cycle number, and α_1, α_2, α_3, α_4; β_1, β_2, β_3; γ_1, γ_2, γ_3 are the respective model parameters. The results show that the proposed ensemble model has the best accuracy for the SoH prediction.

In [32], the authors propose an SoH evaluation method based on capacity estimation. The capacity estimation is made using a sample entropy algorithm based on the voltage responses resulting after the hybrid pulses tests, and on static capacity curves. The sample entropy values are taken as input for the capacity estimation. The sample entropy function can be defined as follows:

$$SampleEn(m, r, N) = -\ln\left[\frac{A^m(r)}{B^m(r)}\right] \tag{10}$$

where N is the length of the sample entropy series, m is the length of a subset of the sample entropy series, for which the difference between any two consecutive elements is bounded by the tolerance r, $A^m(r)$ is the probability that two subsets (vectors) will match $m+1$ elements and $B^m(r)$ is the probability that two subsets will match m elements. The algorithm was tested on multicell batteries at different temperatures. The results show satisfactorily robust estimations.

The battery zero-state hysteresis model is introduced in [33], to predict the changing battery voltage profiles for each charge/discharge cycle. In this case the battery voltage is defined as follows:

$$V_k = OCV(SoC_k) - Ri_k - s_k M \tag{11}$$

where V_k is the battery voltage at battery cycle k, $OCV(SoC_k)$ is the battery open circuit voltage at cycle k, i_k the battery current at cycle k, M and s_k are the hysteresis parameters, with M representing the magnitude and s_k, which depends on the battery current direction, is defined based on a positive value ε as follows:

$$s_k = \begin{cases} 1, & i_k > \varepsilon, \\ -1, & i_k < -\varepsilon, \\ s_{k-1}, & i_k \le |\varepsilon|. \end{cases} \tag{12}$$

2.4. Lifecycle models

The lifecycle models propose another approach to solve the problem of SoH determination of a battery cell. These

battery models monitor battery parameters and their relation with the aging process over the entire lifetime of a battery. The SoH prediction is made based on the observations obtained after extensive offline tests. This approach is different from the other types of models which monitor battery parameters in real time and estimate the SoH based on the instantaneous values of these parameters.

A method for determining the battery aging model has been presented in [34]. Some parameters, such as the operating temperature, DoD, discharge current rate and charge current rate, are analyzed in terms of their impact on the battery health. The proposed model was developed and validated in Matlab.

The authors of [24] propose to monitor battery parameters such as temperature, capacity and number of cycles. In order to predict the SoH, recursive neural network (RNN) and SVM are used. These techniques involve extensive training and high amounts of data to be processed. To shorten the observation time, the authors used accelerated aging tests. It is questionable if these tests can accurately map the real life operating conditions of a battery.

In [35] and [36], the lifecycle models presented are based on battery reliability and failure models. These models are used in addition to data driven techniques in order to estimate the health of the battery. Matlab is used as support for evaluating the model. Because of the extensive laboratory tests, the lifecycle models are generally used in extension with other battery models.

3. SOH ESTIMATION METHODS

The SoH of a battery can be estimated by applying processes and algorithms to its observable parameters, such as the voltage, current and temperature. These processes and algorithms comprise of what we denote as estimation methods, and each method uses a certain battery model as input for transforming the battery observable parameters into SoH and/or RUL. In this section we present some of the most utilized SoH estimation methods that can be found in the art.

3.1. Coulomb counting

Coulomb counting is one of the most common methods used for estimating the SoH. It consists of two steps: in the first step the $Q_{discharge}$ of the battery is determined, corresponding to the value of the SoC of 0%, by integrating the value of discharge current in time; in the second step, the value of the SoH is calculated by dividing the value of $Q_{discharge}$ with the value of the rated capacity:

$$\begin{cases} Q_{discharge} = \int_0^T I(t)dt \\ SoH\ [\%] = \dfrac{Q_{discharge}}{Q_{rated}} \times 100\% \end{cases}. \tag{13}$$

The main battery parameters which are measured and monitored are: battery charge/discharge current, battery voltage, battery charge and battery temperature. This method can be easily converted into an adaptive one, by computing the two values in (13) during each discharge cycle. It was observed, e.g. in [37], that the value of $Q_{discharge}$ is decreasing with the increase of the charge/discharge cycle number. This generates a negative trend for the values of the SoH. Commonly, for a value of the SoH of below 80%, the battery is considered unusable. The accuracy of this method relies on the measurement instruments which should be calibrated periodically.

In [37], authors claim that the accuracy of the coulomb counting method depend primarily on the measurement accuracy of the current and of the initial SoC. A new metric for characterization of the discharge is introduced, depth of discharge (D_{OD}), which is similar to the SoC:

$$D_{OD} = \frac{Q_{released}}{Q_{rated}} \times 100\% \tag{14}$$

where $Q_{released}$ is the discharged battery capacity. At a given instant of time, D_{OD} can be expressed as:

$$\begin{cases} D_{OD}(t) = D_{OD}(t) + \eta \Delta D_{OD}(t) \\ \Delta D_{OD}(t) = \dfrac{-\int_{t_0}^{t_0+\tau} I_b(t)dt}{Q_{rated}} \times 100\% \end{cases} \tag{15}$$

where I_b is the discharge/charge current, η is the operating efficiency. The SoH is defined as the D_{OD} when the battery is exhausted. In each discharge and charge cycle, the D_{OD} is compensated with the charge/discharge efficiency. In addition a recalibration is made at fully charged stage and at fully discharged states. Among the advantages of this solution can be mentioned the low cost implementation of the measurement devices, very low processing power requirements for the algorithms and easy integration [1]. The estimation accuracy depends on the battery charge/discharge cycle, reaching up to 1% for cycle numbers higher than 28.

A complete BMS is presented in [38], in which the SoC and the SoH are computed using coulomb counting. The performance of the standalone coulomb counting method is compared with a modified version which uses OCV in combination with Kalman filtering for SoC estimation. The SoC and SoH estimation errors are computed at different charge currents and the results range between +/− 3%.

3.2. Open circuit voltage (OCV)

The OCV-based method for estimating the SoH of the battery is oriented on defining the SoH as a function of the OCV of the monitored battery. This method is found in the literature both in the offline and in the online form.

As presented in [17], the U_{OCV} is defined based on the simplified electrical model of the battery presented in Figure 3:

$$U_{ocv} = U + IR \tag{16}$$

where, U_{ocv} is the battery OCV, I the battery current, R is the battery internal voltage and U its terminal voltage.

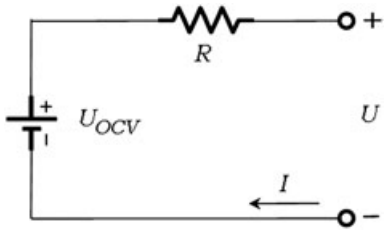

Figure 3. Simplified electrical battery model.

The offline method is based on the mathematical model centered on the OCV value. As presented in the previous section and in [29,30], extensive tests are conducted on the batteries to obtain the OCV curves and a relationship with the battery SoH. In [17], the authors prove the influence of the temperature when building the OCV–SoC curves. This influence should not be neglected, when high accuracy of estimation is needed. The authors provide a method to produce the OCV–SoC curves, including temperature influence and provide validation tests. Despite good accuracy of estimation, the offline approach involves extensive laboratory tests.

The online variant of the method considers OCV as a parameter of the electrical model, which is determined based on system identification. The estimation error is influenced by the initial SoC which is taken into consideration and temperature. When the difference between the real initial SoC and the one used for calculations is kept low, the error is also low. A low battery temperature introduces root-mean-square errors (RMSE) in the range of 5%–25%.

The online OCV method is used in [14], in combination with the parameters of an electrical model, to estimate the SoC and the SoH of the battery. The algorithm presented is suitable for multicell batteries. The estimation is based on power calculations. The estimation inaccuracy depends only on the forecast period, when battery diffusion overvoltage could influence the computed SoC.

In [12], the authors present some disadvantages of using the open current voltage as a parameter for estimating SoH. They claim that this parameter is difficult to determine in practical use. They focus on using an electrical battery model and, based on the CC–CV curves, they try to eliminate the OCV from the equations. This simplifies the algorithms and, thus, reduces the processing power requirements and the hardware costs.

Other authors, [1], consider the OCV method very efficient and simple to use in combination with Coulomb counting. In [30], the authors propose a new OCV model combined with exponential parameters, (6), to estimate SoH with the help of the IC method. This combined approach gives an estimation error of about 1%.

3.3. Impedance spectroscopy method

Electrochemical impedance spectroscopy (EIS) is a method which permits obtaining highly accurate impedance measurements of a battery cell over a large spectrum of frequencies at low currents. The EIS measurements are proven in existing literature to be reliable indicators for a battery SoC and can be used to predict its SoH. Figure 4 shows a typical real and imaginary impedance plot for a battery.

One of the most common usages of the EIS method is to identify the parameters of an electrochemical battery model. This approach is detailed in [20], as the authors develop such an electrochemical battery model based on the specific physical phenomena on Li-ion cells. The model has 16 parameters, out of which six are pre-calculated and deemed fixed, while the remaining 10 are determined using the hybrid multiple particle swarm optimization (HMPSO) method, out of the measured EIS data. The EIS measurements are carried out on Li-ion cells charged at 100% and 50%, in the [0.025 Hz, 4 kHz] frequency range. The identified model is compared against the Randles model using EIS measurements and is demonstrated to be 8 times more accurate than the latter. The paper does not present a complete SoH estimation, but two model parameters are proposed to be used for the estimation.

In [24], the authors couple the EIS method with a RNN in order to predict the SoH and the RUL of the batteries under test. EIS is used as an offline analysis method in this paper as well, to calculate the parameters of the equivalent circuit model proposed by the authors. The ECM contains five elements. Two of them are used to model resistances: the ohmic resistance R_1 and the SoC-dependent resistance R_2. The model also contains two constant phase elements (CPE), namely CPE_1 and CPE_2, which are used to model the diffusion, charge transfer and double layer chemical processes. It has been observed that the CPE_1 and CPE_2 parameters are SoC dependent. The EIS measurements have been conducted at 25 °C and the data has been collected in the frequency spectrum of [0.01 Hz, 10 kHz]. Finally, the model has been validated with a standard current load used for HEVs, thus proving that a relatively simple model is sufficiently accurate and can be used in an on-board BMS.

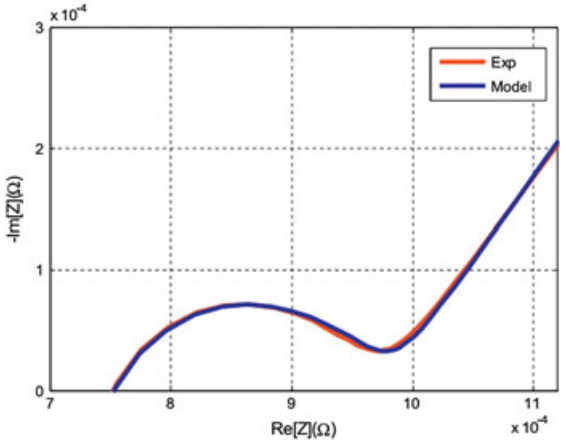

Figure 4. Typical Nyquist plot obtained using EIS [24].

The actual prediction of the remaining battery capacity is performed using a RNN, for which the battery model determined using the EIS method is an input. The algorithm has been used on simulated data, to predict both the battery remaining capacity and its equivalent series resistance (ESR). The average absolute error (calculated from the mean square error (MSE) that the authors provide) is 2.1% for the predicted remaining capacity, which proves the viability and accuracy of the proposed methods.

Another novel application of the EIS method can be seen in [39]. The authors analyze and propose a RUL prediction method for the calendar aging phenomenon of Li-ion cells used in HEVs. The experiments have been performed at three different ambient temperatures and at three SoCs, the EIS measurements proving that the battery SoH is dependent on the temperature and the SoC at which it is used. By analyzing the EIS plots, the authors have identified one parameter, namely the impedance real part at 0.1 Hz, which varies exponentially with the SoH and can thus be used to accurately predict it. Figure 5 demonstrates that the impedance real part can be accurately predicted using the proposed exponential fitting function. The results presented in the paper show that the parameter identified using EIS measurements can be used for robust SoH prediction, and that the model and the process are simpler than those using ECM.

3.4. Kalman filtering

The Kalman filter is a powerful method for estimation of the states of a process. It consists of two parts: the prediction phase and the update phase. In the prediction phase, the process state is estimated. In the update phase, the filter obtains feedback from measurements (affected by Gaussian noise) [40]. The equations of a standard Kalman filter are:

$$\begin{cases} \hat{\mathbf{x}}_{(t|t-1)} = \mathbf{F}_t \hat{\mathbf{x}}_{(t-1|t-1)} + \mathbf{B}_t \mathbf{u}_t \\ \mathbf{P}_{(t|t-1)} = \mathbf{F}_t \mathbf{P}_{(t-1|t-1)} + \mathbf{Q}_t \\ \hat{\mathbf{x}}_{(t|t)} = \hat{\mathbf{x}}_{(t|t-1)} + \mathbf{K}_t \left(\mathbf{y}_t - \mathbf{H}_t \hat{\mathbf{x}}_{(t|t-1)} \right) \\ \mathbf{K}_t = \mathbf{P}_{(t|t-1)} \mathbf{H}_t^T \left(\mathbf{H}_t \mathbf{P}_{(t|t-1)} \mathbf{H}_t^T + \mathbf{R}_t \right)^{-1} \\ \mathbf{P}_{(t|t)} = \mathbf{P}_{(t|t-1)} - \mathbf{K}_t \mathbf{H}_t \mathbf{P}_{(t|t-1)} \end{cases} \quad (17)$$

where $\hat{\mathbf{x}}$ is the estimated state, $\mathbf{F}$ is the state transition matrix, $\mathbf{B}$ is the control matrix, $\mathbf{u}$ is the control vector, $\mathbf{P}$ is the state variance matrix, $\mathbf{Q}$ is the process variance matrix, $\mathbf{y}$ is the measurement vector, $\mathbf{H}$ is the measurement matrix, $\mathbf{K}$ is the Kalman gain and $\mathbf{R}$ is the measurement variance matrix.

The Kalman filter was initially intended for the use in linear systems. For non-linear systems, such as those used for the battery SoH estimation, modified versions of the Kalman filter are proposed in the literature (see Figure 6).

The extended Kalman filter is used for predicting states of a nonlinear process, where the transition and the measurement equations are nonlinear, but need to be differentiable. For battery SoH estimation, the dual extended Kalman filter involves two Kalman filters, one filter is used to predict the SoC and the other one to predict the battery capacity. The unscented Kalman filter (UKF), also known as the sigma point Kalman filter (SPKF), eliminates some of the disadvantages of the extended Kalman filter and improves the estimation. In this case, the probability distribution functions will be estimated by a number of sigma points, which represent a subset of weighted points computed in such way they are close to the mean value. The nonlinear transformation of these points will generate the mean covariance estimate.

In [41] and [42], the authors use a second-order Randles electrical battery model to obtain the state equations of the extended Kalman filter. If in the first case, the SoH is computed based on the SoC; in the second case, the SoH is computed based on the internal battery impedance. The model equations are:

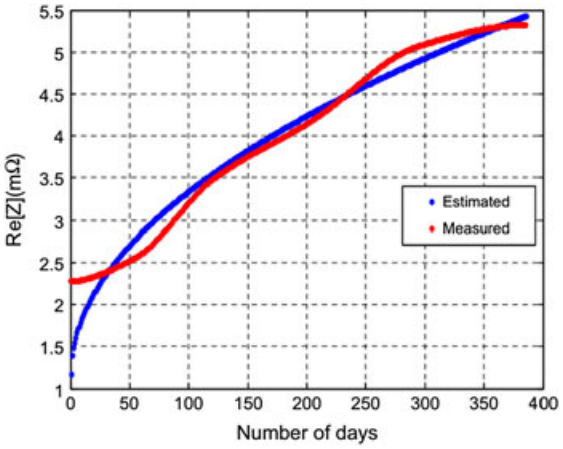

Figure 5. Predicted and measured impedance real part [39].

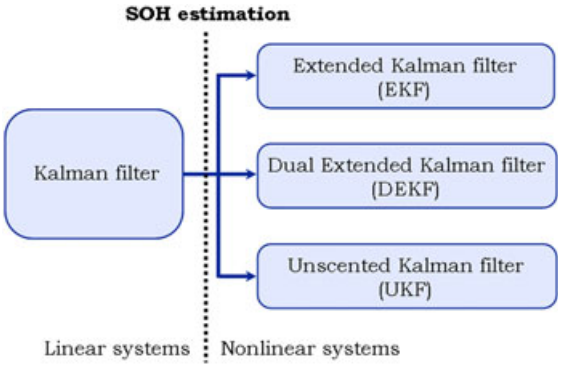

Figure 6. Modified versions of the Kalman filter, used in nonlinear systems.

$$\begin{cases} \begin{pmatrix} SoC_k \\ V_{1,k} \\ V_{2,k} \end{pmatrix} = \begin{pmatrix} 1 & 0 & 0 \\ 0 & 1-\frac{\Delta t}{R_1 C_1} & 0 \\ 0 & 0 & 1-\frac{\Delta t}{R_2 C_2} \end{pmatrix} \begin{pmatrix} SoC_{k-1} \\ V_{1,k-1} \\ V_{2,k-1} \end{pmatrix} + \begin{pmatrix} \frac{\Delta t}{C_{bat}} \\ \frac{\Delta t}{C_1} \\ \frac{\Delta t}{C_1} \end{pmatrix} \\ V_{bat,k} = V_{OC}(SoC_k) + V_{1,k} + V_{2,k} + R_0 I_{bat,k} \end{cases} \tag{18}$$

and, respectively,

$$\begin{cases} \begin{pmatrix} V_{1,k+1} \\ V_{2,k+1} \\ R_{0,k+1} \end{pmatrix} = \begin{pmatrix} e^{\frac{-T}{R_1 C_1}} & 0 & 0 \\ 0 & e^{\frac{-T}{R_2 C_2}} & 0 \\ 0 & 0 & 1 \end{pmatrix} \begin{pmatrix} V_{1,k} \\ V_{2,k} \\ R_{0,k} \end{pmatrix} + \begin{pmatrix} R_1\left(1-e^{\frac{-T}{R_1 C_1}}\right) \\ R_2\left(1-e^{\frac{-T}{R_2 C_2}}\right) \\ 0 \end{pmatrix} I_{bat,k} \\ \left(V_{cell,k} - V_{OC,k}\right)' = (1 \quad 1 \quad 0)x + R_{0,k} I_{bat,k} \end{cases} \tag{19}$$

where SoC_k is the state of charge at time instance k, R_0, R_1, R_2, C_1 and C_2 are the parameters of the second-order Randles which model the battery impedance, $V_{1,k}$ and $V_{2,k}$ are the voltage components measured for the Randles model at instance k, V_{OC} is the battery open circuit voltage, $I_{bat,k}$ the battery current, V_{bat} is the voltage at the battery terminals, $V_{cell,k}$ is the battery terminal voltage at cell level and $x=(V_{1,k}\ V_{2,k}\ R_0\ k)^{\mathrm{T}}$ is the state space variable. In both cases, the reported estimation error has been lower than 4%.

In [43], the extended Kalman filter is used to model LIB parameters, such as the output voltage, OCV and the state of charge. The authors focus on car batteries used in car competitions. The experimental data shows a SoH estimation error below 1%.

The dual extended Kalman filter is presented in [44,45]. Two Kalman filter are used: one to estimate the SoC and the other to estimate the battery parameters, such as the capacity. Figure 7 shows the block diagram of the proposed dual extended Kalman filter. The filter is based on the first-order Randles electrical model. The authors claim that increasing the order of the electrical model makes the estimation hard to implement because of the complexity of operation in real-time applications. In the first paper, the authors use the dual filter in combination with pattern matching resulting in a estimation error of ±5%. The estimation results of the algorithm proposed in the second paper are below 2%.

An UKF is proposed in [46] and [47], for the estimation of the SoH. A second-order Randles model is used as input for the filter equations. The UKF was introduced to address some of the issues of the EKF [48]. Such an issue consists in a high probability of the filter to diverge if the initial state is not specified correctly, resulting in an erroneous model of the process. Another problem is that the approximations of the posterior mean and covariance matrix can introduce large errors and lead to sub-optimal performance.

In [46], the authors compare the performance of the SoH estimation using an UKF with the performance of the coulomb counting method. The UKF adapts perfectly to the nonlinearities of the battery cell characteristics. It overcomes the coulomb counting accumulation errors and the estimated values of the SoC converge approximately to the real value. The estimation error is between 2.2% and 2.9%, depending on the battery cell used.

In [47], the UKF was used in addition with the SVR algorithm. The purpose of SVR is to determine an initial capacity value used as input for the UKF filter. This initial value is estimated offline, based on aging curves. The performance of the algorithms shows an estimation error below 1%.

In [49], the UKF is applied to an electrochemical battery degradation model. The authors monitor the battery voltage response to pulse load cycles and battery internal resistance. The proposed model is adaptive with a measured time of 40 min until the output values converge to the real parameter measurements.

The authors of [50] propose an SoH estimation technique based on a fused algorithm between EKF and quadratic discriminant analysis. The EKF state equations are developed based on the first-order Randles electrical model. The estimated battery parameters obtained by applying the EKF are further used as classification features in the quadratic analysis method. The method was applied considering three classification classes for the batteries: unused,

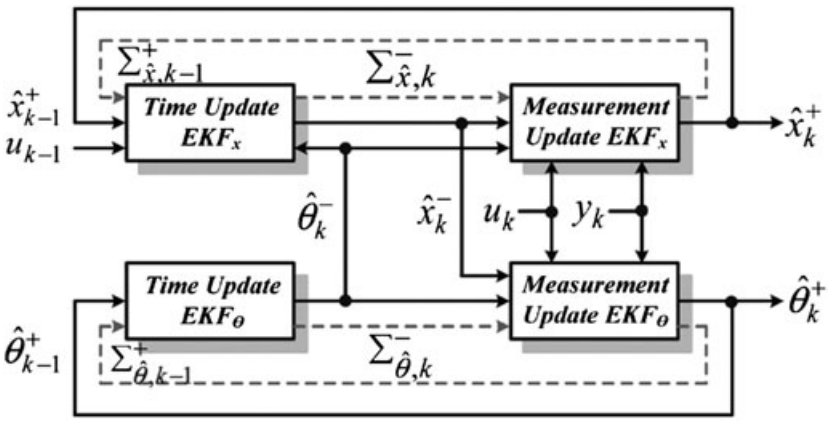

Figure 7. Architecture of the dual extended Kalman filter [44,45].

lightly used and heavily used. The classification error is max. 8.3%.

In [51], the SoH estimation is performed via EKF and a per unit system. Similarly as in [50], the EKF equations are developed using the electrical model of Randles. Three main battery parameters are monitored: R_i, R_{diff} and C_{diff}—where R_i is the internal battery resistance, R_{diff} is the battery diffusion resistance and C_{diff} is the battery diffusion capacitance. All these parameters are derived from the current and voltage measurements. The proposed online method for the SoH estimation is validated using extensive offline measurements of the battery parameters and aging curves. The performance of the algorithm is ±5% compared to the values obtained by ampere-hour counting.

In [52], the authors use a central difference Kalman filter (CDKF) to better estimate the nonlinearities present in the SoH estimation. This is a form of SPKF adapted to practical implementations and therefore has a much lower parameter count.

A novel approach for using the Kalman filter is presented in [53] and [54]. In [53] the authors are using the Kalman filter to update the look-up tables used for the estimation parameters of the battery internal resistance, based on the online battery conditions. The adaptive look-up table update increases the accuracy of the battery aging estimation method. In [54] a new Kalman filtering algorithm is proposed, Adaptive Kalman filter (AKF). The authors claim that the new algorithm provides more robust estimates for the battery parameters.

3.5. SVM—relevance vector machine

The SVM algorithms have become a very popular estimation approach, being introduced in many fields of application and supported by a large community. For battery SoH estimation, the non-linear variant of SVM was adopted by many researchers in this field.

The basic idea of the SVM algorithm is presented in detail in [47] and [55]. Having a set of training data, $\{(x_1, y_1), (x_2, y_2), \ldots, (x_n, y_n)\} \subset R^n \times R$—where R^n is the space of the input data x_i and the target data is y_i, the goal is to find a function $f(x)$ which deviates at most with ε from the targets, for all the training data and which is also as flat as possible. The function has the following form:

$$f(x) = \langle w, x \rangle + b \tag{20}$$

with $w \in R^n$, $b \in R$ and $\langle \cdot\,, \cdot \rangle$ denotes the dot product in R^n. There are situations when such a function does not exist. To overcome this issue, a pair of slack variables, ξ and ξ^*, are introduced, thus allowing a pre-defined interval for the measurement errors. In this case, the problem reduces itself to a dual optimization problem. The dual optimization problem is solved using quadratic programming techniques, which involve a nonlinear mapping to transform the original input (x) to a higher dimensional input feature space. In this case the function becomes:

$$f(x) = \sum_{k=1}^{K} \left(a_k^* - a_k\right) K(x(k), x) + b \tag{21}$$

where a_k^*, a_k are the dual variables obtained by applying the Lagrangian with respect to the primal variables (w, b, ξ, ξ^*), and K is the kernel function (mapping function) with the following form:

$$K(x(k), x(m)) = \langle \Phi(x(k)), \Phi(x(m)) \rangle \tag{22}$$

where Φ represents the nonlinear transformation.

The relevance vector machine (RVM) algorithm [56,57] represents the Bayesian form of the SVM and differs from it by providing a probabilistic interpretation of the outputs. The prediction of the output takes the following form:

$$t = y(x) + \varepsilon_n \tag{23}$$

where t is the predicted target, $y(x)$ is function which translates the input data into the target data as defined in the SVM algorithm and ε_n samples the process noise. After expressing a maximum likelihood function and applying the Bayes rule, the following posterior distribution results:

$$p\left(w|t, \alpha, \sigma^2\right) = \frac{p(t|w, \sigma^2)p(w, \alpha)}{p(t|\alpha, \sigma^2)} \tag{24}$$

where w is a weight vector, α is a hyperparameter vector used to control the deviation of the weights, σ is the variance and p is the posterior distribution function. New data predictions are obtained using the integration of the weights and computing the marginal likelihood of the hyper parameters:

$$\begin{aligned} p(t|\alpha, \sigma^2) &= \int p\left(t|w, \sigma^2\right) p(w|\alpha) dw \\ &= (2\pi)^{N/2} \left|\mathbf{B}^{-1} + \mathbf{\Phi}\mathbf{A}^{-1}\mathbf{\Phi}^T\right|^{-1/2} \\ &\quad \times \exp\left(-\frac{1}{2} t^T \left(\mathbf{B}^{-1} + \mathbf{\Phi}\mathbf{A}^{-1}\mathbf{\Phi}^T\right)^{-1} t\right) \end{aligned} \tag{25}$$

where $\mathbf{A} = \mathrm{diag}(\alpha_1, \ldots, \alpha_{N+1})$, and $\mathbf{B} = \sigma^{-2}\mathbf{I}$, and $\mathbf{\Phi}$ the design matrix of kernel functions, obtained from a set of training data. These two estimation methods, synthesized in (21) and (25) above, can be applied on sets of training data, in which the data represent battery parameters such as the battery capacity.

The SVM algorithms are presented in [29,47,55–60]. As a general characteristic, the algorithms run on high amount of training data gathered offline by cycling the batteries. The online variant of the algorithms are computationally intensive and are presented as Matlab simulations.

In [47], the data used for vector construction is taken from long term battery aging tests. The SVM algorithm is compared with the UKF, providing almost the same prediction errors. When the initial capacity of the battery is known, the prediction error is 1%. Without having information about the initial capacity, the prediction error increases to 20%.

The authors of [58] apply the SVM technique to battery data gathered from impedance spectroscopy tests. The EIS method is based on the Randles electrical circuit. The model estimates the capacity fading and the internal resistance of the battery, which are input for the SoH and RUL calculations. The SVM has better performance than the hidden Markov model method, with an estimation error of 2%.

In [59], the SVM algorithms are applied to battery data provided by the NASA. Two variants of the algorithms are presented: online and combined (online + offline). In the case of the online SVM, the vectors are dynamically updated. The mean absolute estimation error of the SoH is 0.02 in the case of the combined algorithm and 0.03 in the case of the online variant.

SVM applied to data obtained from automated stress tests of hybrid vehicle batteries is discussed in [60]. The support vectors are correlated with the battery load to improve the performance of the algorithms. The MSE obtained is 0.0006, when no load collectors are used, 0.00058 for one load collector configuration and 0.0004, when three load collectors are used.

Application of the SVM for curve fitting of the battery capacity, based on ICA, is presented in [29]. The authors show how to apply the SVR on lithium polymer battery data. They propose an online solution in which the SVMs are updated based on the current battery data and on the offline data (used in the initial stages of estimation). The prediction accuracy of the algorithm is 1% (absolute error).

In [56] and [57], the implementation of RVM is presented. In the first paper, RVM is applied to sample entropy and impedance spectroscopy data provided by NASA for LIBs during charge and discharge cycles. The authors focus on a comparison with the SVM algorithm. The estimation errors are smaller for the RVM method, i.e. below 0.6% (RMSE). The second paper discusses the capacity degradation data of lithium-ion battery used in electric vehicles. Both offline and online RVM algorithms are covered. Here, the authors emphasize on applying the RVM method for the RUL estimation. The estimation error is given in number of battery cycles. The absolute prediction error is below 9 cycles.

3.6. Particle filtering method

The method is best suited for nonlinear systems which are based on a battery model with unknown parameters, or the values of the parameters change with time. The output of the method is an estimation of the probability density function (PDF) based on a set of points (particles), which are values sampled form the state space.

One of the most frequently used algorithms for implementing particle filters is the sampling importance resampling (SIR) [61]. It effectively approximates the resulting probability distribution with a set of weighted particles, while the importance weights of these particles can be approximated as their relative probabilities. The importance weights are relative, so the sum of the weights for a probability distribution is always 1.

In [61], the authors employ a simple electrochemical model of a LIB cell, for which they identify the parameters using an RVM regression method. The values obtained from the RVM regression are used as the initial values to the particle filtering (PF) algorithm. Afterwards, the particles are recalculated, with each measurement iteration. Figure 8 shows a plot of two typical PF prediction results, the RUL PDFs. It can be seen that one of the advantages of using the PF method is that it generates a probability distribution spread out over time, rather than just a single date or point of failure. This clearly conveys the inherent uncertainties in the model and measurements.

The basic particle filter method described above is employed in [62] for estimating the SoC and SoH of lithium iron phosphate ($LiFePO_4$) batteries. The authors use a purely data driven approach, without an explicit battery model, and the only inputs taken into account are the OCV and the current. The resampling step of the PF algorithm is called 'low variance resampling', which is a simplified version of the SIR method described above. In essence, when the new set of samples is generated, the old samples with high weights are multiplied, while old samples with low weights are discarded. The authors validate their algorithm using two battery usage profiles: a photovoltaic off-grid power supply and an electric vehicle driving cycle. The results obtained are not discussed in detail, but the absolute mean error generally falls below 2%. However, the SoH estimation is not described conclusively, because only five to six incomplete battery cycles are analyzed.

The PF method is proved to be more accurate than the statistics-based regression and probabilistic regression methods in [63], by comparing the prediction accuracy and the width of the PDF. Moreover, it is shown that the PF method provides early predictions, as opposed to the other compared methods, which can be used to prevent failures.

The same authors present in [64] an improvement over the classical PF method. They observe that when the state space of the model has large vectors, the resampling process of the PF method cannot acceptably reduce the variance of particle errors. They thus propose to substitute a part of the state space by one analytically computed from another part, naming the new approach the Rao-Blackwellized particle filter (RBPF). By comparing the variances in errors of the PF and RBPF methods, it is shown that the RBPF error variance is much lower than the PF and consequently the PDF is much narrower, yielding an improvement in prediction accuracy.

In [65], the authors propose using two analytical models as inputs for the PF method. More specifically, they employ the PF for estimating the parameters of a polynomial model and an exponential model. The classical PF algorithm of SIR is used and the authors claim that it can be applied online in a BMS. An improvement of this paper is presented by the same authors in [66], although the same PF algorithm is used. A new battery capacity model is introduced, which the authors call an 'ensemble

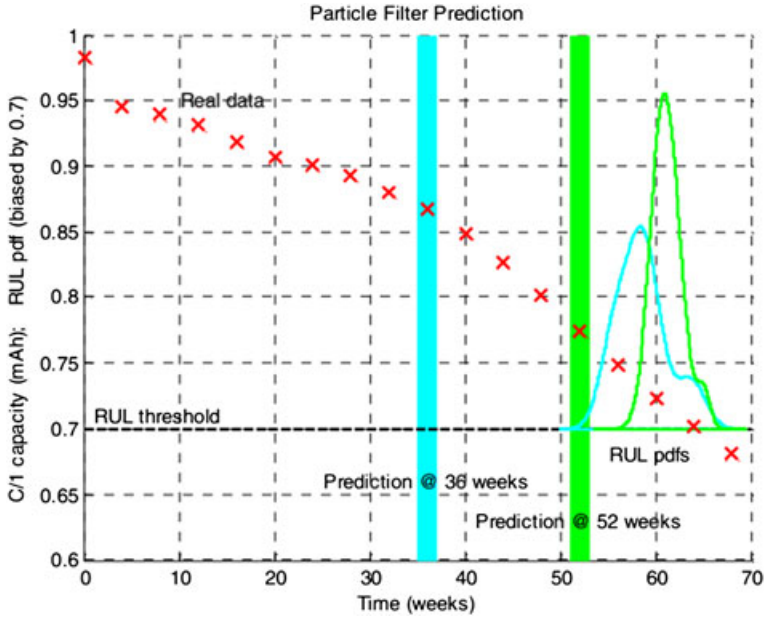

Figure 8. Particle filtering prediction results [61].

model'. It is a fusion of the previous two models and presents a better prediction accuracy than the individual models on which it is based.

The PF method can also be used as an auxiliary mechanism in the prediction of the RUL, as demonstrated in [67]. In this paper, the authors employ a complex data-driven estimation method, based on the Verhulst model. The PSO method is used to improve the model fitting accuracy. The PF is used only to compensate the prediction error by adjusting the parameters of the Verhulst model.

A novel approach to the SoH prediction is introduced in [68] and [69]. The authors employ an empirical mathematical battery model with two exponential terms, which is suitable also for on board implementations. They propose the Bayesian Monte Carlo (BMC) method which is similar to PF. In this regard, its output is the probability distribution function, which is also represented by a sum of samples with associated weights:

$$P(X_k|Q_{0:k}) \approx \sum_{i=1}^{N} \omega_k^i \delta\left(X_k - X_k^i\right) \tag{26}$$

where X_k^i is a set of independent samples from P, which can be selected in practice by using importance sampling; ω_k^i is the importance weight of each sample; $\delta(\cdot)$ is the Dirac (delta) function. The resampling and the weight recalculation methods are different from the classical PF technique. The proposed SoH prediction method uses the Dempster–Shafer theory (DST), which is a data fusion method, to estimate the initial battery model parameters from the training data (the first n battery cycles). BMC is then used to update the model parameters at each cycle, thus updating the SoC and RUL estimations.

A comparison of the proposed method with the EKF method is performed in [68] for one battery type and the results show that this approach yields an estimation error of 1.1%, while the EKF method yields an error of 8.6%. In [69], the authors compare the prediction errors using the same BMC method, but with two different calculation methods of the model parameters. The first method is DST and the second one uses mean averaging to calculate the initial model parameters. It is shown that the DST method is better than the mean averaging method, as the prediction errors at 18 cycles are 2.1 % and 8.3% respectively.

The unscented PF (UPF) method, using the same empirical mathematical model and the same battery data as [68] and [69], is proposed in [62] for estimating the RUL of LIBs. The shortcomings of using the classical PF method (i.e. particle degeneration) are described, along with a theoretical presentation of PF, Kalman filter and UPF. The core idea of the UPF is to use the UKF to generate the proposal distribution of the particles, then to follow the normal PF resampling and weight calculation algorithm. The authors perform a series of tests at different SoH points and conclude that the proposed method yields an absolute error of less than 5%, while applying the standard PF method leads to an error of 7%.

In [70], the authors propose what they call a mutated particle filter (MPF) method for estimating the SoH and RUL. The new method is designed to tackle the shortcomings of the classical, Rao-Blackwellized and UPF methods. Among the most important limitations of the afore-mentioned methods are the sample impoverishment and the failure to accurately capture the PDF. The proposed method transforms the weights of the outlying particles (i.e. the ones which have either very high or very

low weights) so as to represent more accurately the posterior part of the PDF. The process is presented in Figure 9, where (a) represents the posterior distribution with the original particle weights and (b) depicts the same distribution after applying the MPF method. Using an electrochemical lumped-parameter model of a Li-ion cell, the authors evaluate the performance of their proposed method against the classical particle filter and the regularized auxiliary particle filter (RAPF) methods. The reported results indicate that the MPF method achieves a mean RMSE which is 20% lower and an average standard deviation which is 52% lower than that of the classical particle filter method.

In [71], the authors present an implementation of the particle filter method on an embedded platform which can be applied only by using the mean-shift and residual systematic resampling (RSR) to simplify PF operations. A complete RUL estimation and failure detection framework based on particle filters is described in [72]. The framework validation is done using Matlab. In [73], the RUL estimation is determined using the battery capacity. The capacity fade is modeled using a function based on a sum of exponentials. Then, the PF method is applied to this model.

The authors of [62] use particle filter to estimate both SOC and SOH. The battery is modeled using simple electrical model where OCV and internal resistance are two of the model parameters. Monitoring SOC and SOH gives a better insight of battery degradation at each cycle.

In [74], the particle filter is used to approximate the PDF of the available battery power and battery SoC. The novel approach presents an optimization problem for the battery power using a non-linear dynamic model in which the solutions are functions of the battery SoC.

3.7. Fuzzy logic method

Fuzzy logic is a mathematical concept which practically generalizes boolean logic and sets. The core idea is that it allows the members of fuzzy sets to have degrees of membership to that set. A membership function is applied to each member x of a set A and its output is a number in the [0, 1] interval, which represents the degree to which x belongs in the fuzzy set A. Fuzzy logic uses the boolean operators AND, OR and NOT, but it extends their definitions, as presented in Table III.

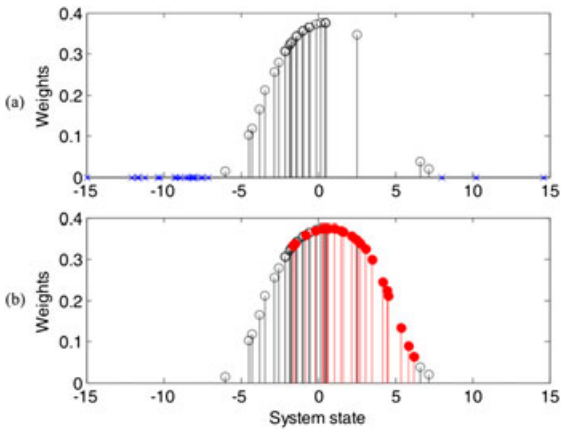

Figure 9. MPF transformation of the system posterior PDF [70].

Fuzzy logic can easily be applied to the battery SoH estimation if we define several output membership functions for the SoH, such as *healthy*, *acceptable* and *not healthy*. However, papers describing the application of the fuzzy logic method to battery SoH estimation have not been encountered in the art until recently.

One of the first papers in which fuzzy logic is used as a viable SoH estimation method is [75]. It proposes a model based approach, utilizing an electrochemical model to extract EIS data and claims that the proposed method can be used for both primary and secondary batteries. The estimation is done for the SoC, SoH and SOL, and is performed using three methods: autoregressive moving-average (ARMA), neural network and fuzzy logic. These methods are compared using the average estimation error and they are also fed into a final decision block, which performs a fusion of the outputs of the three methods and, together with the historical knowledge of the system, outputs the estimation. No detailed description of the fuzzy logic estimator is given, except that it uses four of the input signals, much less than the neural network estimator. The fuzzy logic estimator showed good performance and the results obtained are comparable to the ones obtained using the neural network.

In [76], the authors perform an extended life cycle test on 95 Li–Co batteries, by charging them at a constant 0.5 C current and discharging them at different currents. They employ fuzzy identification based only on measured data to perform SoH estimation. For this, the authors have used three measurable quantities to form the fuzzy sets and the membership functions are of normal distribution type. The reported average error ranges from 1.4% to 9.2%, which proves that the proposed method is suitable for the SoH prediction.

SoH estimation using fuzzy identification is also employed in [77], but using the direct current (DC) resistance as the measured quantity. It is measured during the charging phase and the authors show that there exists an almost linear relationship between the capacity and the DC resistance. After having calculated the average and normalized DC resistance, four membership functions are used to delimit the input range. The output membership functions are actually four thresholds of the health condition: *healthy*, *acceptable*, *weak* and *bad*. The actual calculation of the estimated capacity is done using the

Table III. Definition of fuzzy logic operators.

Operation	Result
x AND y	$\min(x, y)$
x OR y	$\max(x, y)$
NOT x	$1 - x$

defuzzifying formula

$$C_A = \frac{\sum_{i=1}^{4} \mu_i O_i}{\sum_{i=1}^{4} \mu_i} \tag{27}$$

where C_A is the estimated actual capacity, μ_i is the firing strength of the i-th rule and O_i is the firing strength of the output rule. The authors calculate the actual capacity of several batteries having the SoH in the range of 100% to 20% using the proposed fuzzy logic method. They show that the estimation error is less than 5% with the SoH ranging from *healthy* to *weak*, which makes the proposed method better when comparing it to the regression curve method, which is reported to yield estimation errors of around 10%.

A double exponential function, used to model the degradation curve of the battery capacity, is presented in [78]:

$$y_{fit} = a_0 + a_1 e^{-\left(\frac{x}{a_1}\right)^{\beta_1}} + a_2 e^{-\left(\frac{x}{a_2}\right)^{\beta_2}}. \tag{28}$$

The fit function parameters are estimated using fuzzy logic method, the authors reporting a SoH estimation error between 5% and 10%. To decrease this error, neural network estimation is proposed, with the result of reducing the estimation error below 5%. On the other hand, the drawback is that training offline data is needed.

3.8. Other SoH/RUL estimation methods

A novel approach for estimating SOH and RUL, proven suitable for online implementation on resourced constrained embedded platforms, is described [13]. The SOH is estimated based on SOC calculation and a simple least squares regression algorithm is used for prognostics.

In [79], the authors use a novel approach to measure the SoH of sealed lead acid (SLA) batteries. They use **magnetic field** to determine if a battery is degraded or healthy. Two coils are used, one to generate the magnetic field and the second coil to measure the magnetic field changes because of the proton concentration in the battery. Instead of giving some SoH measurement error, the article is focused on the determination of the voltage on the second coil and its relation to the SoH when the battery is healthy and to the SoH when the battery is damaged. The authors do not provide analysis on how this method can be influenced by external magnetic fields, nor do they provide a shielding solution.

A least square method fused with **sample entropy** is presented in [32]. The authors use sample entropy to model the LIB capacity, based on intensive offline tests and a third degree polynomial function to link the capacity with the corresponding sample entropy value at each temperature.

The **approximation entropy** method is described in [80]. This method is an extension of the sample entropy technique used to estimate the SoH for lead-acid batteries and has a better estimation performance. The method consist of computing an $ApEn(m, r, N)$ function for a data sequence $x(i) = x(1), x(2), x(3), \ldots, x(N)$, with N representing the total number of data points, m the length of the subset of data points for which the algorithm runs, r represents the tolerance window, which usually is considered $0.2SD$, and SD represents the standard deviation of the data sequence, defined as

$$SD = \sqrt{\frac{1}{N-1}\sum_{i=1}^{N}\left[x(i) - \frac{1}{N}\sum_{i=1}^{N} x(i)\right]^2}. \tag{29}$$

The $ApEn$ function is computed as follows:

$$ApEn(m, r, N) = \phi^m(r) - \phi^{m+1}(r)$$
$$\phi^m(r) = \frac{1}{N-m+1}\sum_{i=1}^{N}\ln\left(\frac{V^m(i)}{N-m+1}\right)$$
$$V^m(i) = No.of\bar{d}[X(i), X(j)] \leq r$$

and d is the distance between the following vectors (the maximum absolute difference between the scalar components of the vectors):

$$X(i) = [x(i),\ x(i+1),\ \ldots,\ x(i+m-1)],\ i = 1,\ N-m+1$$
$$X(j) = [x(j),\ x(j+1),\ \ldots,\ x(j+m-1)],\ j = 1,\ N-m+1.$$

The author in [81] uses an **unobserved model** to estimate both the SoC and SoH of a LIB. The resulting set of equations is obtained from a complex electrical battery model which uses two RC groups in series. Additionally, a separate electrical model is employed for the battery self-discharge. The SoH estimator has the following form:

$$\dot{\xi} = A\xi + BI_B + D\phi(V_{SOC}, I_B) \tag{30}$$

where A, B and D are state and output matrixes, ξ is the state vector and φ denotes the nonlinearities of the estimation. Based on this state equation the authors compute the internal resistance R_0 of the battery and use the following equation to compute the SoH:

$$SOH = \frac{R_{0,EOF} - R_0}{R_{0,EOF} - R_{0,NEW}} \times 100. \tag{31}$$

In which the R_0 is the current battery internal resistance, $R_{0,EOF}$ is the internal battery resistance when end of life is reached and $R_{0,NEW}$ is the battery internal resistance when the battery is new. The end of life internal resistance value is considered 160% of the resistance value when the battery is new.

In [82], the problem of SoH estimation is addressed based **on PDF** in conjunction with the ICA. The authors focus on different LIBs which have different cyclic voltammogram curves and where the curve fitting is not accurate because of the measurement noise of

voltage/current. Using PDF plots, the SoH evolution can be monitored with high accuracy. To compute the PDF, the authors use the following series:

$$\begin{cases} V_{d,k} = V_0 + k\cdot\delta V \ , \quad k = 0, 1, 2, \ldots \\ Q_{d,n} = Q_0 + n\cdot dQ = n\cdot I\cdot t \ , \quad n = 0, 1, 2, \ldots \end{cases} \tag{32}$$

where $V_{d,k}$ is the sampled digital output voltage of the battery, d is the naming convention for digital, k represents the sample index and $Q_{d,k}$ is the integrated discrete capacity of the battery which corresponds to $V_{d,k}$. These series of values are computed offline by performing multiple charge/discharge cycles.

An adaptation with two PDF functions is described in [83], in the context of adaptive Gaussian mixture model (AGMM). One PDF function is used for historical dataset characterization and the other one is used for current dataset characterization. The algorithm is applied to the capacity parameter of the battery.

The authors in [84] propose the **Gaussian process functional regression** for SoH prognostics. They monitor the battery capacity parameter in order to determine the SoH evolution. The Gauss process is defined as a finite set of random variables $\{f(x_i)|x_i \in X\}$, where x is the input space (the charge/discharge cycles), and a mean and covariance function:

$$\begin{aligned} m(x) &= E(f(x)) \\ k(x_i, x_j) &= E\left[\left(f(x_j) - m(x_j)\right)\cdot\left(f(x_j) - m(x_j)\right)\right]. \end{aligned}$$

The covariance function is composed of a functional part and a model noise part, which is considered Gaussian white noise. The flexibility can be increased by introducing additional parameters, when using linear mean function and quadratic polynomial functions as the mean functions. In this case, the estimation errors are reduced significantly. The algorithm needs a high number of training data sets for increased performance; the authors use a minimum of 100 cycles.

A **Wiener Process with Measurement Error** for RUL estimation is proposed in [85]. The RUL degradation model is represented by the following equation:

$$Y(t) = X(t) + \varepsilon = \lambda t + \sigma_B B(t) + \varepsilon \tag{33}$$

where $Y(t)$ is the degradation process, with the measurement error being taken into consideration, $X(t)$ represents the degradation model without measurement error, ε is the measurement error, λ is the drift parameter, σ_B is the diffusion parameter and $B(t)$ is the standard Brownian motion. The algorithm uses offline parameter estimation combined with an online parameter update process (see Figure 10). The online parameter update is improved by using a heuristic framework for updating the parameters. The authors apply this degradation model to the battery capacity parameter and consider that a battery has reached the end of life when the capacity has faded beyond 20%–30% of the nominal capacity.

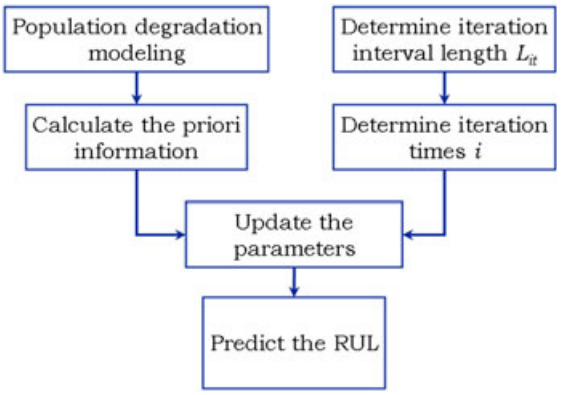

Figure 10. RUL estimation algorithm proposed in [85].

In [86], the authors propose a data driven method based on **autoregressive model** (**AR**) fused with **PSO**. The AR model is optimized by using the PSO algorithm, defined by the following equations:

$$\begin{cases} v_i^{k+1} = w\cdot v_i^k + c_1\left(pbest_i - x_i^k\right) + c_2\left(gbest^k - x_i^k\right) \\ x_i^{k+1} = x_i^k + d\cdot v_i^{k+1} \end{cases} \tag{34}$$

where the first equation represents the velocity update, v_i^{k+1} is the new velocity of particle i, w the inertia weight coefficient, v_i^k is the old velocity of particle i, c_1 and c_2 represent the acceleration constants, d is the tuning parameter (having the value of 1 in almost all cases), x_i^k is the place of particle i at iteration k, x_i^{k+1} is the place of particle i at iteration $k+1$, $pbest_i$ is the best place particle i can have as individual and $gbest$ is the best place of the whole group in the solution space. The PSO is used to determine the AR model order at each step k. To achieve accurate results a limited number of training data is needed.

In [87], a **neural network** is used to model the battery electrochemical properties, having the following activation functions for the neurons in a Gaussian form:

$$\begin{aligned} \varphi_i(r_k) &== G(\|r_k - t_i\|) \\ &= \exp\left(-\frac{\|r_k - t_i\|^2}{\sigma_i^2}\right) \ , \quad i = 1..M \end{aligned} \tag{35}$$

where $r_k = [V_k \ I_k \ SoC_k]^T$ represents the input vector of the neural network at sampling time k, t_i and σ_i are the center and, respectively, the standard deviation for the Gaussian function and M is the number of the neurons in the hidden layer. The neural network outputs the terminal voltage of the time instance $(k+1)$. The SoH is determined based on the voltage–capacity slopes, using an additional fuzzy system. Offline battery cycles are required to train the neural network in order to obtain good estimations.

A structured neural network [42] is used to model nonlinearities of SoH estimation using the battery impedance parameter. The neural network is structured in three main subnetworks: one which uses the SoC, current and temperature measurements to estimate battery voltage and two subnetworks to estimate the R–C parameters of the second-order Randles electrical battery model. The probabilistic neural network is used in [88]. This type of neural network has the advantage of increased learning speed and the training data can be supplied directly without iterations.

In [89] and [90], other **Bayesian approaches** to RUL estimation are presented. The degradation models use capacity curve predictions in a probabilistic way. The estimation is done online, based on offline data, which increases the estimation performance.

In [91,92] and [93] the authors propose a novel method for the estimation of battery SoH based on differential voltage (DV) curves. The main idea of this method is to find the inflection points of the DV curve. This can give an accurate aging estimate when knowing the relationship between the SOH and the DV curve inflection points.

4. EVALUATION AND DISCUSSION OF THE SOH/RUL ESTIMATION METHODS

4.1. Evaluation criteria

In the previous sections we have seen that there are many SoH/RUL estimation methods in the art, each of them targeting specific applications and providing more or less information about their performance. In this section we will perform a structured analysis of all the estimation methods that have been presented up to this point. We thus propose the following six criteria to present a qualitative and quantitative evaluation of the above-mentioned SoH/RUL estimation methods:

- *Battery chemistry*: the chemical structure of the battery cell anode/cathode/electrolyte for which the method is applicable. Although the majority of the presented papers target Li-ion cells with many different anode and cathode chemistries, some of them can also be applied to NiMH or NiCd, while others can be applied to all secondary battery chemistries.
- *Computational complexity*: how suitable is the proposed algorithm to be implemented in a BMS running on an embedded system. The suitability of implementation is inversely proportional to the complexity of the mathematical transformations of the method.
- *Data processing mode*: denotes when the acquired battery parameters are being processed. Offline processing means that the method is applied retroactively, on data which has been previously acquired, while online processing means that the method is applied in real time, as soon as the data is being acquired. There exists also a combination of the two techniques, whereby some battery parameters are processed offline and the others online.
- *Estimation result*: whether the proposed method can be used for estimating only SoH, only RUL or both quantities.
- *Processing time* (if available): The time required for the method to produce the first estimation, from the moment it has sufficient data. Can also represent the average time needed per estimation result, if the estimation is periodically calculated. It is directly dependent on the hardware on which the method is implemented and executed.
- *Estimation precision*: The degree to which the result obtained by applying the method is closer to the actual result. Different metrics are used in the art for expressing the estimation error or precision, such as the absolute error, absolute mean error or RMSE.

4.2. Evaluation of estimation methods

The **Coulomb counting method** is one of the most common methods for the SoH estimation. It can be applied to all battery chemistries, although the works [37] and [38], referenced in Section 3.1, are focused on Li-ion and Li-polymer. The integration of the battery current over time has a low computational complexity, common operations being the addition and the multiplication. As a result, this method is suited for online implementation, even on low power or resource-constrained microcontrollers. The processing times depend on the operation frequency of the microcontroller as well as on the available computation units (arithmetic/logic units). Being a lightweight method, the complexity is moved towards the hardware platform, which is focused on the current measurement. This hardware complexity introduces the need for calibration after several battery charge/discharge cycles.

From the estimation point of view, the method shows a strong dependency between the estimation error and the battery cycle used for this estimation. The estimation performance is relatively low, i.e. below 10%. To increase this estimation performance, the coulomb counting method is used in conjunction with other methods such as the Kalman filtering. In this case the estimation error can be improved to 3%, at the expense of a longer processing time (e.g. 2000 s for the first estimation, as reported in [38]).

The **OCV-based methods** use the relationship between the OCV and the SoH to predict the actual SoH of the battery. These methods can be applied on a wide range of battery chemistries, but for each chemistry, there is a different relation between the OCV and the SoH of the battery. This relationship varies also with the battery cycle. This problem is reduced to finding the relationship between the OCV and the SoH, which can be applied in real-life conditions.

The computational complexity is given by the complexity of the function chosen to express this relationship. A higher complexity gives a better estimation with the

disadvantage of being hard to implement on an embedded target with low processing power. For polynomial functions, the estimation error varies between 5% and 12%. Using exponential terms for polynomial functions the estimation error can be decreased to less than 1%.

Finding the relationship between the OCV and the SoH can be an extensive process which involves performing offline battery charge/discharge cycles. Because of their nature, these techniques are more suited for offline estimation, the online estimation being based on offline data (table lookups).

The **EIS** method is targeted specifically at battery cells having Li-ion based chemistries. The method is rarely used individually for determining the SoH; it is rather used in combination with other methods.

The computational complexity is low when using the standalone method; however it increases when the method is used in combination with a RNN [24]. Data processing is done exclusively offline, because the hardware needed for impedance measurements is too complex to be found in an embedded BMS implementation. Also, performing the measurements requires applying specific current patterns on the battery, which might not be possible during normal online operation.

By applying this method, both SoH and RUL can be obtained. No processing time information is provided in the presented papers. The reported precision is relatively low, with absolute estimation errors ranging from 2% to 10%.

The **PF method** is a data driven technique, and as such it is suitable for all battery chemistries. However, in this survey we analyze the method based on its applicability to various Li-ion based cell chemistries. The mathematical apparatus required for implementing this method uses exponential functions, multiplication and vector/matrix transpositions, thus having a high computational complexity. Data processing is mostly performed online. In other papers the results are obtained by using a combination of offline measurements and parameter identification, as well as online PF processing.

The method is usually employed for determining the RUL, but some papers report estimating the SoH as well. Processing time information is scarce, with only one paper reporting it. The estimation precision varies in the art. Some papers have achieved a very good precision, with results ranging below 1%. Others have presented 3% to 12% error ranges.

Fuzzy logic is a relatively new method to be utilized for SoH/RUL estimation. The method is very versatile, as it has been reported to be used on Li-ion, NiMH and NiCd cell chemistries. It presents a relatively high computational complexity, because its implementation relies on multiplication, division and exponential function terms. Online data processing is an advantage of this method, although it can benefit from offline parameter calculations as well.

All the papers which detail the application of this method focus on the SoH estimation. In general, no processing time information is provided, with the exception of [76], which does present some limited performance data. The estimation precision is average, with reported estimation errors in the range of 1.4% to 10%.

Kalman filtering can be used on multiple cell battery for estimating the SoH. The nature of the method implies a medium to high computational complexity because of the matrix operations combined with exponential terms. This is the reason why very limited implementations on embedded targets are present in the literature; most of the implementations are related to Matlab simulations. The estimation error is lower than the estimation error of the Coulomb counting and the OCV based techniques, being in most cases below 3%. In terms of data processing mode, there are both offline and online variants of the Kalman filtering method.

Machine learning methods (**SVM-RVM**) have a very low estimation error, with values lower than or equal to 1%, in most cases. This precision is achieved because of high computational complexity: exponential functions, vector dot products, etc. This method is suited for the LIB chemistry, but can also be adapted to other chemistries, depending on the battery model used. This method can be used both online and offline. Because of its complexity, a very low number of implementations are currently available.

The data-driven approach based on **least squares** is suited for embedded platforms with scarce resources. It can be used for the SOH estimation of all battery types. The algorithm complexity is low because it involves only basic multiplications and additions. Another advantage is the low execution time, of the order of hundreds of microseconds per battery cycle on a minimum 10-MHz core. Among the drawbacks of the method is the high estimation error in the case of nonlinear slope of the SOH degradation curve.

Magnetic field-based method is a new approach to determine the SoH in a noninvasive way. It was intended to be used for lead acid batteries. The main advantage of this kind of method is the computational complexity with is limited to simple linear equations in which the magnetic field is computed.

Sample entropy and **approximate entropy** methods are suited for all chemistries. They have a good estimation precision, with an absolute error of about 2% and can be modified to run online, offline or in a combination of the two. The main disadvantage is the high computational complexity needed to run these methods; vector/matrix operations and exponential functions are needed for this type of estimator.

The **unobserved model** is used to estimate the SoH of LIBs. This online method uses offline data training to estimate system parameters. The absolute error of the estimation converges to ~0% after 4000 s of running the algorithm; in the first 681 s it is higher than 21.2% and decreases gradually to 6.7% after 1000 s, 3% after 2000 s and 0.6% after 3000 s. The estimation error converges to 0 with an acceptable rate. From the computational complexity point of view, this method uses vector and matrix

operations, having parameters in exponential form. This gives a high computational complexity.

PDF can be used to monitor the SoH on LIBs. The relation between the SoH and PDF curves is computed offline; in this case an online solution has to be modeled in such way it will use the offline data. The advantage of using PDF to estimate the SoH is given by the simpler way of using the PDF curves which are more accurate than using curve fitting algorithms which need high accuracy measurements of current and voltage yielding to higher costs. The estimation error of this method is below 2% with medium to high computational complexity: function derivatives can be expressed by using subtraction of the function members. The offline characterization of the batteries, based on extensive battery tests, can be mentioned as an important disadvantage of this technique.

Gaussian process functional regression for SoH prognostics is one of the accurate estimation methods for LIBs. The main advantage is the reduction of cost and complexity of the particle filter method, by using a prediction approach. Estimation errors of less than 0.5% are obtained by using medium to high computational complexity given by logarithmic, exponential functions and matrix operations. The method can be fitted to an online and offline approach, extensive training data has to be performed in order to obtain high precision estimations. The flexibility

Table IV. Evaluation of the Coulomb counting and OCV methods.

Method	Refs	Battery chemistry	Computational complexity	Data processing mode	SoH/RUL estim.	Processing time for first estimation	Estimation precision
Coulomb counting	[37]	Li-ion	Linear functions and operations	Online	SoH	N/A	~9% in 21th cycle; ~1% after 8th cycle
	[38]	LiFePO4	Linear functions and operations (standalone method); matrix operation (multiplication, transpose), exponential functions (modified version of method)	Online	SoH	In extension with Kalman filtering process for experimental data: 2000 s	Between +/−3%
Open circuit voltage (OCV)	[17]	Li-ion	Linear operations: Matrix operation (multiplication, transpose)	Offline and online	SoH	N/A	<5% in most of the cases when temperature is taken into account; >5% when the initial SoC is between 45% and 65%
	[14]	Li-ion	Linear operations	Online	SoH	Implemented on a low cost 16 bit microcontroller; processor load: 60%	RMSE: 4%–20% for the constant current case; for constant power: 5%–12%
	[12]	Li-ion	Linear operations, exponential functions	Online with parameters obtained offline	SoH	N/A	Estimation error: <1%
	[30]	Li-ion	Polynomial functions with exponential terms	Parameter identification offline	SoH	N/A	<1%

DOI: 10.1002/er

Table V. Evaluation of the Kalman filtering based SoH/RUL estimation methods.

Method	Refs	Battery chemistry	Computational complexity	Data processing mode	SoH/RUL estim.	Processing time for first estimation	Estimation precision
Kalman filtering	[50]	Apply to all; demonstrated for NiMH	Matrix operation (multiplication, transpose), log function	Offline	SoH	N/A	Max. 8.3%
	[51]	Li-ion	Matrix operation (multiplication, transpose), square root function	Offline	SoH	N/A	Estimation error in range of +/−5%
	[46]	Li-ion	Matrix operation (multiplication, transpose), polynomial functions (3rd order)	Online based on offline data	SoH	N/A	RMS ranges between 2.2% and 2.9%
	[44]	Li-ion	Matrix operation (multiplication, transpose)	Online	SoH	N/A	Estimation error in range of +/−5%
	[41]	Li-ion	Matrix operation (multiplication, transpose), exponential function	Online	SoH	Estimation based on data acquired over 30-min interval	Parameter model estimation error 1%; SoH estimation error: <4%
	[47]	Li-ion	Matrix operation (multiplication, transpose), exponential function	Online	SoH	N/A	Estimation error: <1%
	[42]	Li-ion	Matrix operation (multiplication, transpose), exponential function	Offline	SoH	N/A	Estimation error: <4%
	[43]	Li-ion	Matrix operation (multiplication, transpose), exponential function	Online with parameters obtained offline	SoH	N/A	Estimation error: <1%
	[45]	Lead acid	Matrix operation (multiplication, transpose), exponential function	Online	SoH	N/A	<2%
	[49]	Li-ion	Matrix operation (multiplication, transpose), Linear operations,	Online	SoH	Update of the model parameters in order to have an acceptable estimation error range, requires 40 min	2%
	[52]	Li-ion	Matrix operation (multiplication, transpose), square root function	Online	SoH	N/A	Mean error ranges between −0.6 and 0.6

DOI: 10.1002/er

Table VI. Evaluation of the machine learning (SVM-RVM) estimation methods.

Method	Refs	Battery chemistry	Computational complexity	Data processing mode	SoH/RUL estim.	Processing time for first estimation	Estimation precision
Machine learning (SVM-RVM)	[29]	Li-Polymer	Exponential functions, vector dot product (multiply and accumulate); authors state as 'moderate'	Online based on offline data	SoH	Specified moderate computational load	Absolute prediction error: 1%
	[47]	Apply to all; demonstrated for NMC (Nickel Manganese Cobalt)	Exponential functions, vector dot product (multiply and accumulate)	Offline	SoH	N/A	Estimation error: <1%
	[58]	Li-ion	Exponential functions, vector dot product (multiply and accumulate)	Offline (can be adapted online)	SoH and RUL	Specified that the algorithm is CPU intensive	~2%
	[56]	Li	Exponential functions, vector dot product (multiply and accumulate), matrix operations (transpose, multiplication)	Offline	SoH	N/A	Missing data for first battery cycle; SVM RMSE between 0.47 and 1.43; RVM RMSE between $5.96 \cdot 10^{-5}$ and 0.5
	[59]	Li	Exponential functions, vector dot product (multiply and accumulate)	Online and combined (online + offline)	RUL	N/A	Combined approach: MAE 0.02; online approach: MAE 0.03
	[60]	Li-ion	Exponential functions, vector dot product (multiply and accumulate)	Online based on offline data	SoH and RUL	N/A	Conventional use: MSE $8 \cdot 10^{-4}$; 1LC: MSE $0.1 \cdot 10^{-4}$; 3LC: MSE $0.02 \cdot 10^{-4}$
	[57]	Li-ion	Exponential functions, vector dot product (multiply and accumulate), matrix operations (transpose, multiplication)	Online based on offline data	RUL	N/A	Absolute prediction error after 100 cycles: 4 cycles; absolute prediction error after 200 cycles: 2 cycles

DOI: 10.1002/er

Table VII. Evaluation of the particle filtering based SOH/RUL estimation methods.

Method	Refs	Battery chemistry	Computational complexity	Data processing mode	SoH/RUL estim.	Processing time for first estimation	Estimation precision
Particle filtering	[63]	Graphite anode lithium nickel cobalt oxide cathode	Exponential functions	Offline (RVM regression) and online (particle filtering)	RUL	N/A	9.1% at week 32 of 64; 4.0% at week 48 of 64
	[64]	Graphite anode lithium nickel cobalt oxide cathode	Exponential functions, floating point multiplication	Offline (RVM regression) and online (particle filtering)	RUL	N/A	3.1% at testing week 48 of 64
	[65]	Li-ion	Exponential functions (model A), multiplications (model B)	Online	SoH and RUL	N/A	Model A: 0.4% at cycle 550 of 780; model B: 11.5% at cycle 550 of 780
	[66]	Li-ion	Exponential functions, multiplication	Online	RUL	N/A	For Cell #01: 12.1% at cycle 566 of 849; for Cell #02: 1.5% at cycle 428 of 643; for Cell #V4: 0.1% at cycle 422 of 633
	[67]	Li-ion	Exponential functions, division	Online	RUL	N/A	For cell A4: 4.2% at cycle 27 of 48; for cell A2: 1.6% at cycle 120 of 189
	[68]	Graphite anode lithium cobalt oxide cathode	Exponential functions, floating point multiplication, vector transposition	Can be processed online	SoH and RUL	10 ms on an Intel Core i7 M60 2.67 GB processor and 4 GB RAM (Matlab)	2.1% at cycle 18 of 48; 1.1% at cycle 250 of 610
	[69]	Li-ion	Exponential functions, multiplication	Offline and online	RUL	N/A	2.0% at cycle 18 of 48
	[62]	LiFePO4	Trigonometric functions, floating point multiplication	Offline and online	SoH	N/A	<2.0%, but few cycles are analyzed
	[100]	Graphite anode lithium cobalt oxide cathode	Exponential functions, floating point multiplication, vector transposition	Offline and online	RUL	N/A	<5%

Int. J. Energy Res. (2016) © 2016 John Wiley & Sons, Ltd.
DOI: 10.1002/er

of the method permits estimation of SoH in the presence of the regeneration phenomenon which is usually found in the case of LIBs, while other estimation methods can be negatively affected by its presence.

Wiener process-based method can be applied to predict the RUL of LIBs. The degradation model focuses on battery capacity parameter. A practical implementation was conducted on NASA battery data and the MSE was used to determine the algorithm accuracy. The MSE is high on first cycles when the initial parameter estimation has relative high errors, but it decreases below 1 after 65th – 67th cycle, when the heuristic parameter update has high accuracy. Despite a very good estimation accuracy, this method has a high computational complexity given by the use of matrix and vector operations combined with logarithmic and exponential functions. Another disadvantage represents the offline parameter computation which requires some training data.

The **AR with PSO** method can achieve very good results for RUL estimation of LIBs. It is applied to the capacity parameter of the battery. The estimation errors are less than 10 cycles when the input dataset contains no more than 120 points and can reach one to two cycles for larger datasets, e.g. 190 data points. The advantage of using this method is its reduced computational complexity because of the linear equations. It is known that using an autoregressive method implies heavy training data but the combination with the PSO algorithm reduces the quantity of training data at minimum. The algorithm has also a reduced processing time, e.g. ~2 s are needed for the estimation of the RUL on an Intel processor with 3 GHz.

SoH estimation using **neural networks** can be used for all types of battery chemistries. The method is very accurate having a maximum estimation of 2% (using 100 training samples). The algorithm is computationally intensive, using exponential functions, vector and matrix operations. The method supports the online mode only, based on offline data.

The **Bayesian approach** used for estimating the RUL of LIB has very good estimation results but the implementation is difficult because of its high computational complexity. Very good results can be obtained using this method: the error can be reduced to 0.2%–0.3% when offline data is used in conjunction with online samples.

The **DV curve** methods provide highly accurate battery SoH estimation results, with the estimation error ranging between 2 and 3%. The estimation can be made online and offline, with medium to low computational power requirements.

A detailed synopsis of the evaluation results for the state of the art battery SoH/RUL estimation methods, according to the previously presented criteria, is provided in Tables IV–IX.

Table VIII. Evaluation of the fuzzy logic and impedance spectroscopy methods.

Method	Refs	Battery chemistry	Computational complexity	Data processing mode	SoH/RUL estim.	Processing time or first estimation	Estimation precision
Fuzzy logic	[75]	Primary Li secondary NiCd and NiMH	N/A	Offline and online	SoH	N/A	Between 2.0% and 7.9% for SoC; N/A for SoH
	[76]	Graphite anode lithium cobalt oxide cathode	Exponential functions, multiplication, division	Online	SoH	15.6 ms on an unspecified computer	Between 1.4% and 9.2%
	[77]	Li-ion	Multiplication, division	Online	SoH	N/A	Max. 5%
Impedance spectroscopy	[20]	Li-ion	*No algorithm for directly determining the SoH is presented	Offline	SoH and RUL	N/A	N/A
	[24]	Graphite anode lithium cobalt manganese nickel oxide cathode	Exponential function, RNN with 13 neurons	Offline	SoH and RUL	N/A	Average 2.1%
	[39]	Graphite anode lithium cobalt manganese nickel oxide cathode	*No algorithm for directly determining the SoH is presented	Offline	SoH and RUL	N/A	Max 10% (for the predicted impedance real part)

Table IX. Comparative evaluation of the other SOH/RUL estimation methods.

Method	Refs	Battery chemistry	Computational complexity	Data processing mode	SoH/RUL estim.	Processing time for first estimation	Estimation precision
Data driven least squares regression	[13]	NiMH	Simple linear equations	Online	SoH and RUL	<550 μs at 14 MHz on ARM 7 embedded platform	Estimation error: +/− 5 cycles
Magnetic field	[79]	SLA	Simple linear equations	Online	SoH	N/A	N/A (gives only correlation between SoH and magnetic field)
Least squares fused with sample entropy	[32]	Li-ion	Vector operations, logarithmic function	Online, based on offline data	SoH	N/A	Average relative error 2%
Approx. entropy	[80]	Lead acid	Vector operation, matrix operation, logarithmic functions	Online, based on offline data	SoH	N/A	N/A
Unobserved model	[81]	Li-ion	Vector and matrix operations, exponential function	Online, based on offline data	SoH	N/A	Absolute error: >21.2% before 681 s, 6.7% after 1000 s, 3% after 2000 s, 0.6 % after 3000 s, ~0% after 4000 s, but only a few cycles are considered
PDF	[82]	$LiMn_2O_4$ $LiFePO_4$	Linear functions, derivative functions, probabilities	Online based on offline data	SoH	N/A	Estimation error under 2%
GPR/GPFR	[84]	Li-ion	Matrix operation, function derivatives, logarithmic and exponential expressions	Offline, can be modified to online, based on offline data	SoH	N/A	MAPE: <0.5% RMSE: 1.5–6
Wiener Process	[85]	Li-ion	Exponential and logarithmic expressions, vector and matrix operations	Online, based on offline data	RUL	N/A	MSE: <1 after cycle 67
AR with PSO	[86]	Li-ion	Linear expressions	Online, with minimum training data	RUL	<2 s for first prediction, ~2 s for prediction	Estimation error of remaining cycles:

(*Continues*)

Table IX. (Continued)

Method	Refs	Battery chemistry	Computational complexity	Data processing mode	SoH/RUL estim.	Processing time for first estimation	Estimation precision
						with 190 samples as input, on an Intel Core E5800, 3 Ghz, 2 GB RAM	<30 cycles in first 120 cycles, <2 cycles when estimation is done between 120 and 200 cycles
Neural network	[87]	VRLA	Exponential functions, matrix and vector operations	Online	SoH	N/A	Estimation error of max. 2%
	[42]	Li-ion	Exponential functions, matrix and vector operations	Online, based on offline data	SoH	N/A	Estimation error: <0.5%
	[88]	Li-ion	Exponential functions, matrix and vector operations	Online, based on offline data	SoH	N/A	Average error of 0.28% for a number of 2000 training samples
Bayesian approach	[89]	Li-ion	Vector operations, exponential functions	Online	RUL	N/A	Estimation error below 2%
	[90]	Li-ion	Vector operations, exponential functions	Online	RUL	N/A	Estimation error between 0.3% and 10%

5. COMMERCIAL SOLUTIONS FOR THE SOH ESTIMATION

Battery powered devices experienced a tremendous growth in the past years which has determined the boorn of a new semiconductor market niche: the battery fuel gauges. Some of the most prominent semiconductor companies, which provide such integrated circuits/solutions, are Texas Instruments, Maxim Integrated, Linear Technology, ST Microelectronics and HDM Systems.

A battery fuel gauge is an integrated circuit which has several features: measurement of battery system parameters such as current, voltage and temperature, SoC determination and SoH determination. In most of the cases the battery fuel gauges need external circuitry in order to operate. A block schematic of this circuitry is presented in Figure 11.

Besides the positive and negative terminals (P+ and P−), the battery can have a third terminal (T) if the temperature sensor resides inside the pack. An external thermistor can be externally applied, if no internal sensor is presented. A battery protection circuit is needed to safeguard the battery from overvoltage, overcurrent or high temperature condition. The protection circuit must decouple the battery pack from the rest of the system in case of an unwanted event is present. The battery charger is used to provide the charge voltage when the battery pack is in charge mode and system voltage if the battery pack is in discharge mode. It has to be chosen based on the electrical characteristics of the battery pack and the system components.

The battery fuel gauge is the most important component. Based on the battery state, it controls the battery charger and informs periodically the microcontroller system about the battery state via specific interface (usually SMBUS or I2C). The microcontroller system stores all the information from the battery fuel gauge and controls its mode of operation. It can control all the fuel gauge configuration registers available.

Products like the ST Microelectronics STC3105 [94], or Linear Technology LTC2941 [95] do not expose information related to SoH/RUL of the battery. They only provide information about battery SoC and in this case the user can build up its own SoH estimation algorithm using

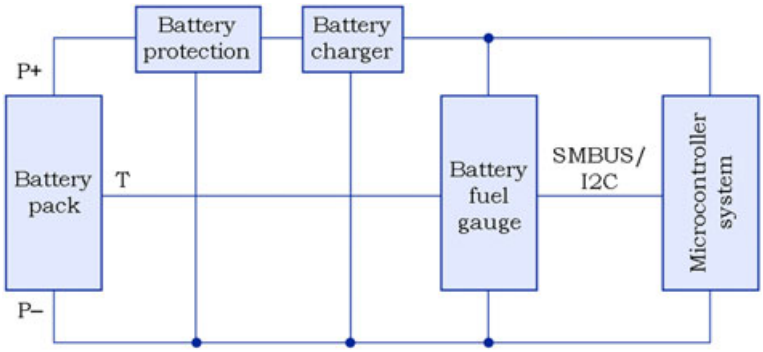

Figure 11. Battery fuel gauge circuit schematics.

Table X. Comparison of commercial solutions for battery fuel gauge and SoH estimation.

Product	Refs	Battery chemistry	Computational complexity	Data processing mode	SoH/RUL estimation	Processing time for first estimation	Estimation precision
TI Bq27531	[96,97]	Li-ion (older versions support a wide range)	Hardware	Online	SoH	1 s	1%
MAX17047	[98]	Li-ion	Hardware	Online	SoH	N/A	<2%
HDM BFG-24-S	[99]	Lead-acid	Hardware	Online	SoH	N/A	5%

all the battery parameters which are provided by the circuit. The user can configure the fuel gauge parameters such as charge/discharge thresholds, battery charge termination and battery alerts.

Texas Instruments bq27531 [96] is a fuel gauge designed for LIBs which uses Texas Instruments Impedance Track technology for battery management [97]. It implements an electrical battery model which monitors the OCV of the battery. The user is able to configure the gauge parameters based on the technical specification from the battery manufacturer: input voltage, input current, designed capacity, battery limits, charge termination timer intervals, thermal compensation, charging voltage, which can be set as a function of temperature (five points can be stored in the non-volatile memory), and charging profile for different charging rates (five steps).

This fuel gauge provides information about the SoH of the battery. The 'StateOfHealth' register is available and the data is expressed in percentage (0 – 100%). The manufacturer gives little information about how the value in the register is computed. The value is based on the ratio between the 'Full Charge' capacity and the 'Designed' capacity. The 'Full Charge' capacity used in the calculation is an estimation of the full charge capacity at 25 °C and the full charge capacity corresponding to the current SoH at the 'LoadI' register. The manufacturer claims an estimation error of 1% in most of the operating conditions. To achieve this, the user should know how to configure the chip. The user should also know the battery parameters from the battery manufacturer. Older versions of Texas Instruments bq product use coulomb counting for the SoC determination, thus supporting a wide range of battery chemistries: NiMH, lead-acid and Li-ion.

Similarly to the previous product, the Maxim Integrated MAX17047 [98] computes the SoH based on SoC. The SoC determination algorithm is a mix between coulomb counting and OCV. The OCV is used to reduce the errors introduced by the need of coulomb counting calibration. The SoH value is given by the 'Age' register which is the ratio between the 'FullCAP' register and 'DesignCap' register. Here, the 'FullCAP' register stores the actual value of the charging capacity sampled at the moment of charge termination. The estimation error is under 2%.

The HDM Systems BFG-24-S fuel gauge [99] is designed for lead-acid battery chemistry. The SoH is computed based on the ratio between the total AHr for a fully charged battery and the designed capacity (given by the battery manufacturer). The full charge capacity is computed based on coulomb counting method. The estimation error is 5%.

Table X summarizes the comparison of the most relevant off-the-shelf commercial devices for battery fuel gauge and SoH estimation.

6. CONCLUSIONS

There is a multitude of battery models and methods in the field of battery SOH estimation, ranging from the simplest to implement, to very complex ones, which require high

computational resources. As a consequence, a large number of papers discussing this topic have been published in the art and some of the most relevant are analyzed in this review.

The presented models and methods are very heterogeneous, making it hard to objectively analyze and compare them. A comprehensive set of clear and measurable criteria has been defined in order to sort out this problem.

Considering the precision of the estimation, we have found that, although the more complex methods generally present a lower estimation error, there are also several relatively simple methods that provide good precision. However, the main drawback of using simple methods is that these lower ranges of errors are achieved only in case of stable operating conditions and low variance of battery parameters. On the other hand, the more complex methods cover almost all possible battery life degradation scenarios. For instance, most of the simple solutions do not take into account the variation of battery temperature or are defined only for a fixed value, e.g. 25 °C.

Our evaluation revealed that only a small number of papers which present complex methods have a practical implementation on embedded targets, most of them being only validated in simulation environments, such as Matlab.

The most complex techniques, such as the PF, Kalman filtering and SVR, have an estimation error in the range of 1% to 2%, while the other present large and very large estimation errors in comparable scenarios.

The existing commercial solutions usually implement the simpler methods and offer a wide range of configurability, making them relatively easy to integrate into a BMS, compared to more theoretical approaches.

NOMENCLATURE

AGMM = Adaptive Gaussian mixture model
AR = Autoregressive model
ARMA = Autoregressive moving-average
BEV = Battery electrical vehicle
BMC = Bayesian Monte Carlo
BMS = Battery management system
CC–CV = Constant current–constant voltage
CDKF = Central difference Kalman filter
DEKF = Dual extended Kalman filter
DoD = Depth of discharge
DST = Dempster–Shafer theory
ECM = Equivalent circuit model
EIS = Electrochemical impedance spectroscopy
EKF = Extended Kalman filter
ESR = Equivalent series resistance
HEV = Hybrid electrical vehicle
HMPSO = Hybrid multiple particle swarm optimization
ICA = Incremental capacity analysis
KF = Kalman filter
LIB = Li-ion battery
$LiFePO_4$ = Lithium iron phosphate
MPF = Mutated particle filter
MAE = Mean absolute error
MAPE = Mean absolute percentage error
MSE = Mean square error
NiMH = Nickel-metal-hydride
OCV = Open circuit voltage
PDF = Probability density function
PF = Particle filtering
PHM = Prognostics and health management
PSO = Particle swarm optimization
RAPF = Regularized auxiliary particle filter
RBPF = Rao-Blackwellized particle filter
RMSE = Root-mean-square error
RNN = Recursive neural network
RRT = Remaining run time
RSR = Residual systematic resampling
RUL = Remaining useful life
RVM = Relevance vector machine
SIR = Sampling importance resampling
SLA = Sealed lead acid
SPKF = Sigma point Kalman filter
SOA = Safe operating area
SoC = State of charge
SoF = State of function
SoH = State of health
SVM = Support vector machine
SVR = Support vector regression
UKF = Unscented Kalman filter
UPF = Unscented particle filtering
VRLA = Valve-regulated lead-acid

ACKNOWLEDGEMENTS

This work was supported by a grant of the Romanian National Authority for Scientific Research and Innovation, CNCS – UEFISCDI, project number PN-II-RU-TE-2014-4-0731.

REFERENCES

1. Waag W, Fleischer C, Sauer DU. Critical review of the methods for monitoring of lithium-ion batteries in electric and hybrid vehicles. *Journal of Power Sources* 2014; **258**:321–339. doi:10.1016/j.jpowsour.2014.02.064.
2. Lu L, Han X, Li J, Hua J, Ouyang M. A review on the key issues for lithium-ion battery management in electric vehicles. *Journal of Power Sources* 2013; **226**:272–288. doi:10.1016/j.jpowsour.2012.10.060.
3. Rezvanizaniani SM, Liu Z, Chen Y, Lee J. Review and recent advances in battery health monitoring and prognostics technologies for electric vehicle (EV) safety and mobility. *Journal of Power Sources*

2014; **256**:110–124. doi:10.1016/j.jpowsour.2014.01.085.
4. Price B, Richardson J, Dietz E. State-of-charge and state-of-health monitoring: implications for industry, academia, and the consumer. *Proceedings IEEE Electro/Information Technology*, 2012, 1–6. DOI: 10.1109/EIT.2012.6220713.
5. Zhang J, Lee J. A review on prognostics and health monitoring of Li-ion battery. *Journal of Power Sources* 2011; **196**:6007–6014. doi:10.1016/j.jpowsour.2011.03.101.
6. Si XS, Wang W, Hu CH, Zhou DH. Remaining useful life estimation: a review on the statistical data driven approaches. *European Journal of Operational Research* 2011; **213**:1–14. doi:10.1016/j.ejor.2010.11.018.
7. Barre A, Deguilhem B, Grolleau S, Gerard M, Suard F, Riu D. A review on lithium-ion battery ageing mechanisms and estimations for automotive applications. *Journal of Power Sources* 2013; **241**:680–689. doi:10.1016/j.jpowsour.2013.05.040.
8. Hatzell KB, Sharma A, Fathy HK. A survey of long-term health modeling, estimation, and control of lithium-ion batteries: challenges and opportunities. *Proceedings American Control Conference*, 2012; 584–591. DOI: 10.1109/ACC.2012.6315578.
9. Liao L, Kottig F. Review of hybrid prognostics approaches for remaining useful life prediction of engineered systems, and an application to battery life prediction. *IEEE Transaction on Reliability* 2014; **63** (1). doi:10.1109/TR.2014.2299152.
10. Seaman A, Dao TS, McPhee J. A survey of mathematics-based equivalent-circuit and electrochemical battery models for hybrid and electric vehicle simulation. *Journal of Power Sources* 2014; **256**:410–423. doi:10.1016/j.jpowsour.2014.01.057.
11. Moldovan AN, Weibelzahl S, Muntean CH. Energy-aware mobile learning: opportunities and challenges. *IEEE Communications Survey & Tutorials* 2014; **16** (1):234–265. doi:10.1109/SURV.2013.071913.00194.
12. Guo Z, Qiu X, Hou G, Liaw BY, Zhang C. State of health estimation for lithium ion batteries based on charging curves. *Journal of Power Sources* 2014; **249**:457–462. doi:10.1016/j.jpowsour.2013.10.114.
13. Micea MV, Ungurean L, Carstoiu GN, Groza V. Online state-of-health assessment for battery management systems. *IEEE Transactions on Instrumentation and Measurement* 2011; **60** (6):1997–2006. doi:10.1109/TIM.2011.2115630.
14. Waag W, Fleischer C, Sauer DU. Adaptive on-line prediction of the available power of lithium-ion batteries. *Journal of Power Sources* 2013; **242**:548–559. doi:10.1016/j.jpowsour.2013.05.111.
15. Ranjbar AH, Banaei A, Khoobroo A, Fahimi B. Online estimation of state of charge in Li-ion batteries using impulse response concept. *IEEE Transaction on Smart Grid* 2012; **3**(1):360–367. doi:10.1109/TSG.2011.2169818.
16. Tsang KM, Sun L, Chan WL. Identification and modelling of lithium ion battery. *Energy Conversion and Management* 2010; **51**:2857–2862. doi:10.1016/j.enconman.2010.06.024.
17. Xing Y, He W, Pecht M, Tsui KL. State of charge estimation of lithium-ion batteries using the open-circuit voltage at various ambient temperatures. *Applied Energistics* 2014; **113**:106–115. doi:10.1016/j.apenergy.2013.07.008.
18. Remmlinger J, Buchholz M, Meiler M, Bernreuter P, Dietmayer K. State-of-health monitoring of lithium-ion batteries in electric vehicles by on-board internal resistance estimation. *Journal of Power Sources* 2011; **196**:5357–5363. doi:10.1016/j.jpowsour.2010.08.035.
19. Chen Z, Mi CC, Fu Y, Xu J, Gong X. Online battery state of health estimation based on genetic algorithm for electric and hybrid vehicle applications. *Journal of Power Sources* 2013; **240**:184–192. doi:10.1016/j.jpowsour.2013.03.158.
20. Li SE, Wang B, Peng H, Hu X. An electrochemistry-based impedance model for lithium-ion batteries. *Journal of Power Sources* 2014; **258**:9–18. doi:10.1016/j.jpowsour.2014.02.045.
21. Prasad GK, Rahn CD. Model based identification of aging parameters in lithium ion batteries. *Journal of Power Sources* 2013; **232**:79–85. doi:10.1016/j.jpowsour.2013.01.041.
22. Ecker M, Gerschler JB, Vogel J, Kabitz S, Hust F, Dechent P, Sauer DU. Development of a lifetime prediction model for lithium-ion batteries based on extended accelerated aging test data. *Journal of Power Sources* 2012; **215**:248–257. doi:10.1016/j.jpowsour.2012.05.012.
23. Stevanatto LC, Brusamarello VJ, Tairov S. Parameter identification and analysis of uncertainties in measurements of lead–acid batteries. *IEEE Transaction on Instrument Measurement* 2014; **63**(4):761–768. doi:10.1109/TIM.2013.2283545.
24. Eddahech A, Briat O, Bertrand N, Deletage JY, Vinassa JM. Behavior and state-of-health monitoring of Li-ion batteries using impedance spectroscopy and recurrent neural networks. *International Journal of Electrical & Power Energy Systems* 2012; **42**:487–494. doi:10.1016/j.ijepes.2012.04.050.
25. Moura SJ, Chaturvedi NA, Krstic M. PDE estimation techniques for advanced battery management systems —part II: SOH identification. *Proceedings IEEE*

American Control Conference, 2012; 566–571. DOI: 10.1109/ACC.2012.6315020.
26. Moura SJ, Chaturvedi NA, Krstic M. PDE estimation techniques for advanced battery management systems —I: SOC estimation. *Proceedings IEEE American Control Conference*, 2012; 559–565. DOI: 10.1109/ACC.2012.6315019.
27. Santhanagopalan S, White RE. State of charge estimation using an unscented filter for high power lithium ion cells. *International Journal of Energy Research* 2010; **34**:152–163. doi:10.1002/er.1655.
28. Eddahech A, Briat O, Vinassa JM. Determination of lithium-ion battery state-of-health based on constant-voltage charge phase. *Journal of Power Sources* 2014; **258**:218–227. doi:10.1016/j.jpowsour.2014.02.020.
29. Weng C, Cui Y, Sun J, Peng H. On-board state of health monitoring of lithium-ion batteries using incremental capacity analysis with support vector regression. *Journal on Power Sources* 2013; **235**:36–44. doi:10.1016/j.jpowsour.2013.02.012.
30. Weng C, Sun J, Peng H. A unified open-circuit-voltage model of lithium-ion batteries for state-of-charge estimation and state-of-health monitoring. *Journal of Power Sources* 2014; **258**:228–237. doi:10.1016/j.jpowsour.2014.02.026.
31. Xing Y, Ma EWM, Tsui KL, Pecht M. An ensemble model for predicting the remaining useful performance of lithium-ion batteries. *Microelectronics Reliability* 2013; **53**(6):811–820. doi:10.1016/j.microrel.2012.12.003.
32. Hu X, Li SE, Jia Z, Egardt B. Enhanced sample entropy-based health management of Li-ion battery for electrified vehicles. *Energy* 2014; **64**:953–960. doi:10.1016/j.energy.2013.11.061.
33. Mastali M, Vazquez-Arenas J, Fraser R, Fowler M, Afshar S, Stevens M. Battery state of the charge estimation using Kalman filtering. *Journal of Power Sources* 2013; **239**:294–307. doi:10.1016/j.jpowsour.2013.03.131.
34. Omar N, Monem MA, Firouz Y, Salminen J, Smekens J, Hegazy O, Gaulous H, Mulder G, Van den Bossche P, Coosemans T, Van Mierlo J. Lithium iron phosphate based battery—assessment of the aging parameters and development of cycle life model. *Applied Energistics* 2014; **113**:1575–1585. doi:10.1016/j.apenergy.2013.09.003.
35. Xing Y, Miao Q, Tsui KL, Pecht M. Prognostics and health monitoring for lithium-ion battery. *Proceedings IEEE Intelligence and Security Informatics*, 2011, 242–247. DOI: 10.1109/ISI.2011.5984090.
36. Penna JAM, Nascimento CL Jr., Rodrigues LR. Health monitoring and remaining useful life estimation of lithium-ion aeronautical batteries. *Proceedings*. *IEEE Aerospace*, 2012, 1–12. DOI: 10.1109/AERO.2012.6187375.
37. Ng KS, Moo CS, Chen YP, Hsieh YC. Enhanced Coulomb counting method for estimating state-of-charge and state-of-health of lithium-ion batteries. *Applied Energistics* 2009; **86**:1506–1511. doi:10.1016/j.apenergy.2008.11.021.
38. Divakar BP, Cheng KWE, Wu HJ, Xu J, Ma HB, Ting W, Ding K, Choi WF, BF Huang, CH Leung. Battery management system and control strategy for hybrid and electric vehicle. *Proceedings Power Electronics Systems and Applications*, 2009; 1–6.
39. Eddahech A, Briat O, Woirgard E, Vinassa JM. Remaining useful life prediction of lithium batteries in calendar ageing for automotive applications. *Microelectronics Reliability* 2012; **52**:2438–2442. doi:10.1016/j.microrel.2012.06.085.
40. Saxena A. Subject MI63: Kalman filter tank filling. *Cornell Univ*., 2008, (Available from: http://www.cs.cornell.edu/courses/cs4758/2012sp/materials/mi63slides.pdf) Accessed on 2016.04.12.
41. Rosca B, Kessels JTBA, Bergveld HJ, van den Bosch PPJ. On-line parameter, state-of-charge and aging estimation of Li-ion batteries. *Proceedings IEEE Vehicle Power and Propulsion Conference*, 2012; 1122–1127. DOI: 10.1109/VPPC.2012.6422617.
42. Andre D, Nuhic A, Soczka-Guth T, Sauer DU. Comparative study of a structured neural network and an extended Kalman filter for state of health determination of lithium-ion batteries in hybrid electric vehicles. *Engineering Applications of Artificial Intelligence* 2013; **26**:951–961. doi:10.1016/j.engappai.2012.09.013.
43. Daboussy M, Chrenko D, Aglzim EG, Che Daud ZH, Le Moyne L. Characterisation of a commercial automotive lithium ion battery using extended Kalman filter. *Proceedings IEEE Transportation and Electrification Conference and Expo*, 2013; 1–6. DOI: 10.1109/ITEC.2013.6574522.
44. Kim J, Lee S, Cho BH. Complementary cooperation algorithm based on DEKF combined with pattern recognition for SOC/capacity estimation and SOH prediction. *IEEE Transactions on Power Electronics* 2012; **27**(1):436–451. doi:10.1109/TPEL.2011.2158554.
45. Dragicevic T, Sucic S, Guerrero JM. Battery state-of-charge and parameter estimation algorithm based on Kalman filter. *Proceedings IEEE Europe Conference*, 2013; 1519–1524. DOI: 10.1109/EUROCON.2013.6625179.

46. Pivlelait B, Rentel C, Plett GL, Marcel M, Carmen D. An advanced battery management system for lithium ion batteries. *Proceedings Ground Vehicle Systems Engineering and Technology Symposium* 2011; 1–7.
47. Andre D, Appel C, Soczka-Guth T, Sauer DU. Advanced mathematical methods of SOC and SOH estimation for lithium-ion batteries. *Journal of Power Sources* 2013; **224**:20–27. doi:10.1016/j.jpowsour.2012.10.001.
48. Wan EA, Van Der Merwe R. The unscented Kalman filter for nonlinear estimation. Proceedings IEEE Adaptive Systems for Signal Processing, Communications, and Control, 2000; 153–158. DOI: 10.1109/ASSPCC.2000.882463.
49. Bole B, Kulkarni CS, Daigle M. Adaptation of an electrochemistry-based Li-ion battery model to account for deterioration observed under randomized use. *Proceedings Prognostics and Health Management 14*, 2014; 1−9.
50. Barlak C, Ozkazanc Y. A classification based methodology for estimation of state-of-health of rechargeable batteries. *Proceedings IEEE Electrical and Electronics Engineering*, 2009; II.101–II.105.
51. Kim J, Cho BH. State-of-charge estimation and state-of-health prediction of a Li-ion degraded battery based on an EKF combined with a per-unit system. *IEEE Transactions on Vehicular Technology* 2011; **60**(9). doi:10.1109/TVT.2011.2168987.
52. Remmlinger J, Buchholz M, Soczka-Guth T, Dietmayer K. On-board state-of-health monitoring of lithium-ion batteries using linear parameter-varying models. *Journal of Power Sources* 2013; **239**:689–695. doi:10.1016/j.jpowsour.2012.11.102.
53. Fridholm B, Wik T, Nilsson M. Kalman filter for adaptive learning of look-up tables with application to automotive battery resistance estimation. *Control Engineering Practice* 2016; **48**:78–86. doi:10.1016/j.conengprac.2015.12.021.
54. Fridholm B, Wik T, Nilsson M. Robust recursive impedance estimation for automotive lithium-ion batteries. *Journal of Power Sources* 2016; **304**:33–41. doi:10.1016/j.jpowsour.2015.11.033.
55. Smola AJ, Scholkopf B. A tutorial on support vector regression. *Statistics Computing* 2004; **14**(3):199–222. doi:10.1023/B:STCO.0000035301.49549.88.
56. Widodo A, Shim MC, Caesarendra W, Yang BS. Intelligent prognostics for battery health monitoring based on sample entropy. *Expert Systems with Applications* 2011; **38**:11763–11769. doi:10.1016/j.eswa.2011.03.063.
57. Wang D, Miao Q, Pecht M. Prognostics of lithium-ion batteries based on relevance vectors and a conditional three-parameter capacity degradation model. *Journal of Power Sources* 2013; **239**:253–264. doi:10.1016/j.jpowsour.2013.03.129.
58. Pattipati B, Sankavaram C, Pattipati KR. System identification and estimation framework for pivotal automotive battery management system characteristics. *IEEE Transactions on Systems Man Cybernetics C* 2011; **41**(6):869–884. doi:10.1109/TSMCC.2010.2089979.
59. Zhou J, Liu D, Peng Y, Peng X. Dynamic battery remaining useful life estimation: an on-line data-driven approach. *Proceedings IEEE Instrumentation and Measurement Technology Conference*, 2012; 2196–2199. DOI: 10.1109/I2MTC.2012.6229280.
60. Nuhic A, Terzimehic T, Soczka-Guth T, Buchholz M, Dietmayer K. Health diagnosis and remaining useful life prognostics of lithium-ion batteries using data-driven methods. *Journal of Power Sources* 2013; **239**:680–688. doi:10.1016/j.jpowsour.2012.11.146.
61. Saha B, Goebel K, Poll S, Christophersen J. An integrated approach to battery health monitoring using Bayesian regression and state estimation. *Proceedings IEEE Autotestcon*, 2007; 646–653. DOI: 10.1109/AUTEST.2007.4374280.
62. Schwunk S, Armbruster N, Straub S, Kehl J, Vetter M. Particle filter for state of charge and state of health estimation for lithium–iron phosphate batteries. *Journal of Power Sources* 2013; **239**:705–710. doi:10.1016/j.jpowsour.2012.10.058.
63. Goebel K, Saha B, Saxena A, Celaya JR, Christophersen JP. Prognostics in battery health management. *IEEE Instrumentation & Measurement Magazine* 2008; **11**(4):33–40. doi:10.1109/MIM.2008.4579269.
64. Saha B, Goebel K, Poll S, Christophersen J. Prognostics methods for battery health monitoring using a Bayesian framework. *IEEE Instrumentation & Measurement Magazine* 2009; **58**(2):291–296. doi:10.1109/TIM.2008.2005965.
65. Xing Y, Ma EWM, Tsui KL, Pecht M. A case study on battery life prediction using particle filtering. *Proceedings IEEE Prognostics and System Health Management*, 2012; 1–6. DOI: 10.1109/PHM.2012.6228847.
66. Xing Y, Ma EWM, Tsui KL, Pecht M. An ensemble model for predicting the remaining useful performance of lithium-ion batteries. *Microelectronics Reliability* 2013; **53**:811–820. doi:10.1016/j.microrel.2012.12.003.
67. Xian W, Long B, Li M, Wang H. Prognostics of lithium-ion batteries based on the Verhulst model, particle swarm optimization and particle filter. *IEEE Transactions on Instrumentation and*

Measurement 2014; **63**(1):2–17. doi:10.1109/TIM.2013.2276473.
68. He W, Williard N, Osterman M, Pecht M. Prognostics of lithium-ion batteries based on Dempster–Shafer theory and the Bayesian Monte Carlo method. *Journal of Power Sources* 2011; **196**:10314–10321. doi:10.1016/j.jpowsour.2011.08.040.
69. He W, Williard N, Osterman M, Pecht M. Remaining useful performance analysis of batteries. *Proceedings IEEE Prognostics and Health Management*, 2011; 1–6. DOI: 10.1109/ICPHM.2011.6024341.
70. Li DZ, Wang W, Ismail F. A mutated particle filter technique for system state estimation and battery life prediction. *IEEE Transactions on Instrumentation and Measurement* 2014; **63**(8):2034–2043. doi:10.1109/TIM.2014.2303534.
71. Li G, Li B, Liu Z, Chen X. Implementation and optimization of particle filter tracking algorithm on multi-DSPs system. *Proceedings IEEE Cybernetics Intelligent Systems*, 2008; 152–157. DOI: 10.1109/ICCIS.2008.4670761.
72. Orchard ME, Tang L, Vachtsevanos G. A combined anomaly detection and failure prognosis approach for estimation of remaining useful life in energy storage devices. *Proceedings Prognostics and Health Management 11*, 2011; 1−7.
73. Chen C, Pecht M.Prognostics of lithium-ion batteries using model-based and data-driven methods. *Proceedings Prognostics and Health Management*, 2012; 1–6. DOI: 10.1109/PHM.2012.6228850.
74. Burgos-Mellado C, Orchard ME, Kazerani M, Cardenas R, Saez D. Particle-filtering-based estimation of maximum available power state in lithium-ion batteries. *Applied Energy* 2016; **161**:349–363. doi:10.1016/j.apenergy.2015.09.092.
75. Kozlowski JD. Electrochemical cell prognostics using online impedance measurements and model-based data fusion techniques. *Proceedings IEEE Aerospace*, 2003; 3257–3270. DOI: 10.1109/AERO.2003.1234169.
76. Lin HT, Liang TJ, Chen SM. The state-of-health diagnosis of Li–Co batteries with fuzzy identification. *Proceedings IEEE Power Electronics and Motion Control Conference*, 2012; 2678–2682. 10.1109/IPEMC.2012.6259285.
77. Tsang KM, Chan WL. State of health detection for lithium ion batteries in photovoltaic system. *Energy Conversion and Management* 2013; **65**:7–12. doi:10.1016/j.enconman.2012.07.006.
78. Landi M, Gross G. Measurement techniques for online battery state of health estimation in vehicle-to-grid applications. *IEEE Transactions on Instrumentation and Measurement* 2014; **63**(5):1224–1234. doi:10.1109/TIM.2013.2292318.
79. Khare N, Singh P, Vassiliou JK. A novel magnetic field probing technique for determining state of health of sealed lead-acid batteries. *Journal of Power Sources* 2012; **218**:462–473. doi:10.1016/j.jpowsour.2012.06.085.
80. Sun YH, Jou HL, Wu JC, Wu KD. Auxiliary health diagnosis method for lead-acid battery. *Applied Energistics* 2010; **87**:3691–3698. doi:10.1016/j.apenergy.2010.04.013.
81. Gholizadeh M, Salmasi FR. Estimation of state of charge, unknown nonlinearities, and state of health of a lithium-ion battery based on a comprehensive unobservable model. *IEEE Transactions in Industrial Electronics* 2014; **61**(3):1335–1344. doi:10.1109/TIE.2013.2259779.
82. Feng X, Li J, Ouyang M, Lu L, Li J, He X. Using probability density function to evaluate the state of health of lithium-ion batteries. *Journal of Power Sources* 2013; **232**:209–218. doi:10.1016/j.jpowsour.2013.01.018.
83. Yu J. Health degradation detection and monitoring of lithium-ion battery based on adaptive learning method. *IEEE Transactions on Instrumentation and Measurement* 2014; **63**(7):1709–1721. doi:10.1109/TIM.2013.2293234.
84. Liu D, Pang J, Zhou J, Peng Y, Pecht M. Prognostics for state of health estimation of lithium-ion batteries based on combination Gaussian process functional regression. *Microelectronics Reliability* 2013; **53**:832–839. doi:10.1016/j.microrel.2013.03.010.
85. Tang S, Yu C, Wang X, Guo X, Si X. Remaining useful life prediction of lithium-ion batteries based on the wiener process with measurement error. *Energies* 2014; **7**:520–547. doi:10.3390/en7020520.
86. Long B, Xian W, Jiang L, Liu Z. An improved autoregressive model by particle swarm optimization for prognostics of lithium-ion batteries. *Microelectronics Reliability* 2013; **53**:821–831. doi:10.1016/j.microrel.2013.01.006.
87. Shahriari M, Farrokhi M. Online state-of-health estimation of VRLA batteries using state of charge. *IEEE Transaction on Industrial Electronics* 2013; **60**(1):191–202. doi:10.1109/TIE.2012.2186771.
88. Lin HT, Liang TJ, Chen SM. Estimation of battery state of health using probabilistic neural network. *IEEE Transactions on Industrial Informatics* 2013; **9**(2):679–685. doi:10.1109/TII.2012.2222650.
89. Jin G, Matthews DE, Zhou Z. A Bayesian framework for on-line degradation assessment and residual life prediction of secondary batteries in spacecraft. *Reliability Engineering & System Safety* 2013; **113**:7–20. doi:10.1016/j.ress.2012.12.011.

90. Ng SSY, Xing Y, Tsui KL. A naive bayes model for robust remaining useful life prediction of lithium-ion battery. *Applied Energistics* 2014; **118**:114–123. doi:10.1016/j.apenergy.2013.12.020.
91. Wang L, Pan C, Liu L, Cheng Y, Zhao X. On-board state of health estimation of LiFePO4 battery pack through differential voltage analysis. *Applied Energy* 2016; **168**:465–472. doi:10.1016/j.apenergy.2016.01.125.
92. Torai S, Nakagomi M, Yoshitake S, Yamaguchi S, Oyama N. State-of-health estimation of LiFePO4/graphite batteries based on a model using differential capacity. *Journal of Power Sources* 2016; **306**:62–69. doi:10.1016/j.jpowsour.2015.11.070.
93. Berecibar M, Garmendia M, Gandiaga I, Crego J, Villareal I. State of health estimation algorithm of LiFePO4 battery packs based on differential voltage curves for battery management system application. *Energy* 2016; **103**:784–796. doi:10.1016/j.energy.2016.02.163.
94. STMicroelectronics. STC3105: battery monitor Ic with alarm output for gas gauge applications. *Datasheet*, 2011. Available from: http://www.st.com/st-web-ui/static/active/en/resource/technical/document/datasheet/DM00037883.pdf. [Accessed on 12 April 2016].
95. Linear Technology. LTC2941 battery gas gauge with I2C interface. *Datasheet*, 2010. Available from: http://cds.linear.com/docs/en/datasheet/2941fa.pdf. [Accessed on 12 April 2016].
96. Texas Instruments. bq27531-G1 battery management unit impedance track fuel gauge with MaxLife technology for use with the bq2419x charger controller. *Datasheet*, 2015. Available from: http://www.ti.com/lit/ds/symlink/bq27531-g1.pdf). [Accessed on 12 April 2016].
97. Yu M, Barsukov Y, Vega M. Theory and implementation of impedance track battery fuel-gauging algorithm in bq2750x family. *Texas Instruments Appl. Report*, SLUA450, 2008. Available from: http://www.ti.com/lit/an/slua450/slua450.pdf. [Accessed on 12 April 2016].
98. Maxim Integrated. MAX17047/MAX17050: ModelGauge m3 fuel gauge. *Datasheet*, 2015, (Available from: https://www.maximintegrated.com/en/products/power/battery-management/MAX17050.html#popuppdf). [Accessed on 12 April 2016].
99. HDM Systems. BFG-24-S battery fuel gauge product specification. *Datasheet*, 2009. Available from: http://www.hdm-sys.com/pdf/hdm_manual_bfg.pdf. [Accessed on 12 April 2016].
100. Miao Q, Xie L, Cui H, Liang W, Pecht M. Remaining useful life prediction of lithium-ion battery with unscented particle filter technique. *Microelectronics Reliability* 2013; **53**:805–810. doi:10.1016/j.microrel.2012.12.004."